

BEAM DIAGNOSTICS

CAS 2008; Dourdan, France; A. Hofmann

May/June 2008

- 1) E.M. FIELDS USED FOR DIAGNOSTICS**
- 2) TRANSVERSE EFFECTS**
- 3) LONGITUDINAL EFFECTS**
- 4) COLLECTIVE EFFECTS**

Concentrate on:

circular machines, bunched beams, high energy,
relation between beam dynamics and diagnostics.

1) E.M. FIELDS USED FOR DIAGNOSTICS

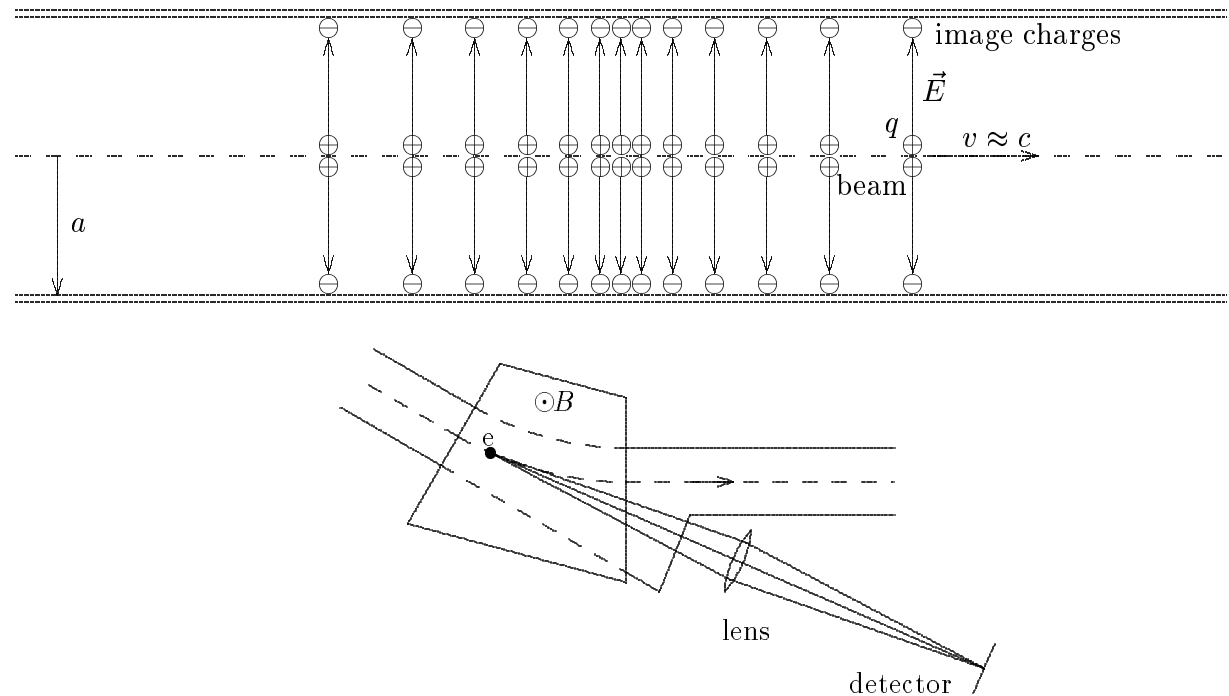
Beam diagnostics uses electromagnetic fields \vec{E} and \vec{B} created by the beam. We distinguish 'near field' attached to charges and 'far'- or "' radiation field' propagating.

The near field:

It is a Lorentz transformed Coulomb field, electric field concentrated in the transverse direction, induces wall currents in chamber which are used to measure the beam with a monitor.

The radiation field:

Fields above the cut-off frequency $\omega > \omega_{\text{cut-off}}$ can propagate in chamber. As synchrotron radiation they are used for diagnostics to measure beam at the source.

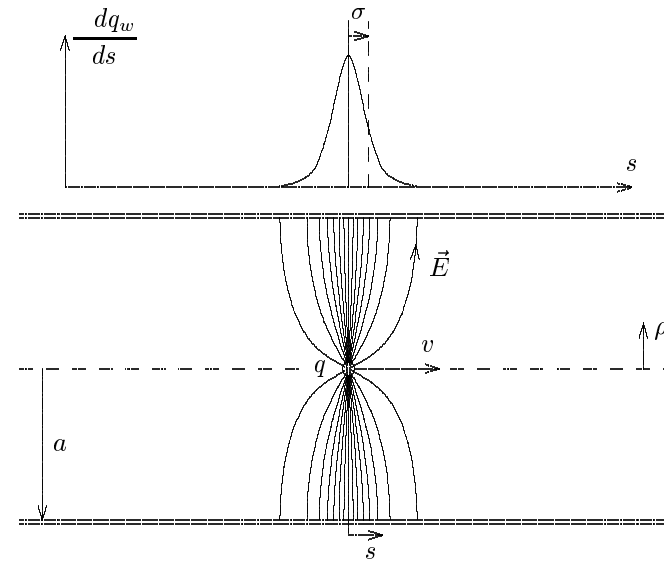


The E -field of a point charge induces surface charges of opposite sign on a circular chamber of radius a with Lorentz contracted distribution dq_w/ds of RMS width

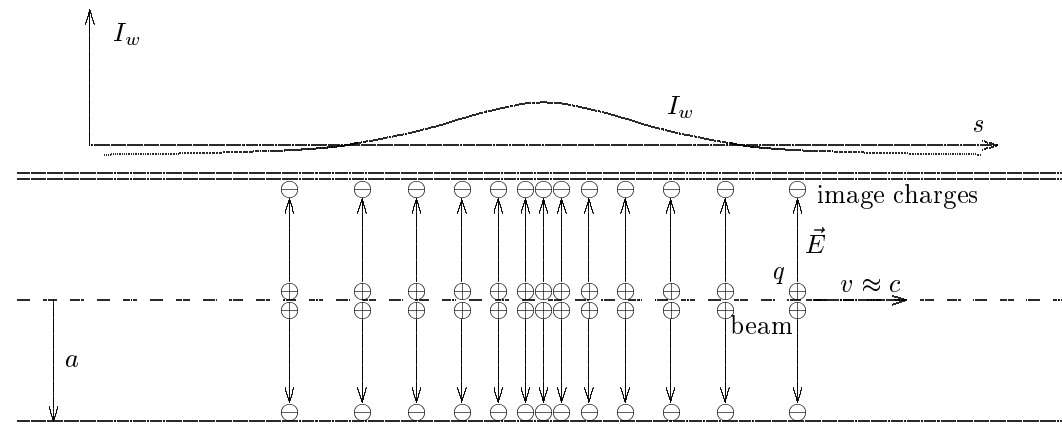
$$\sigma_w = \frac{a}{\sqrt{2}\gamma}$$

being very small for $\gamma \gg 1$.

Charges induced by a bunch current $I(t)$ have nearly the same distribution but wall current does not contain DC-part, an uniform beam induces an uniform static charge which does not move $I_w(t) = -(I(t) - \langle I \rangle)$.

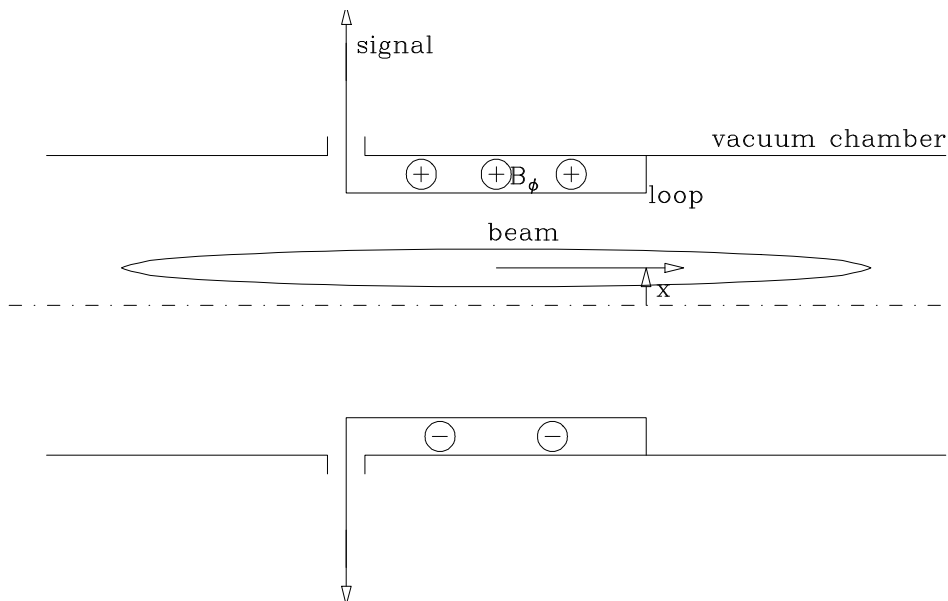


Induced charges by a moving proton

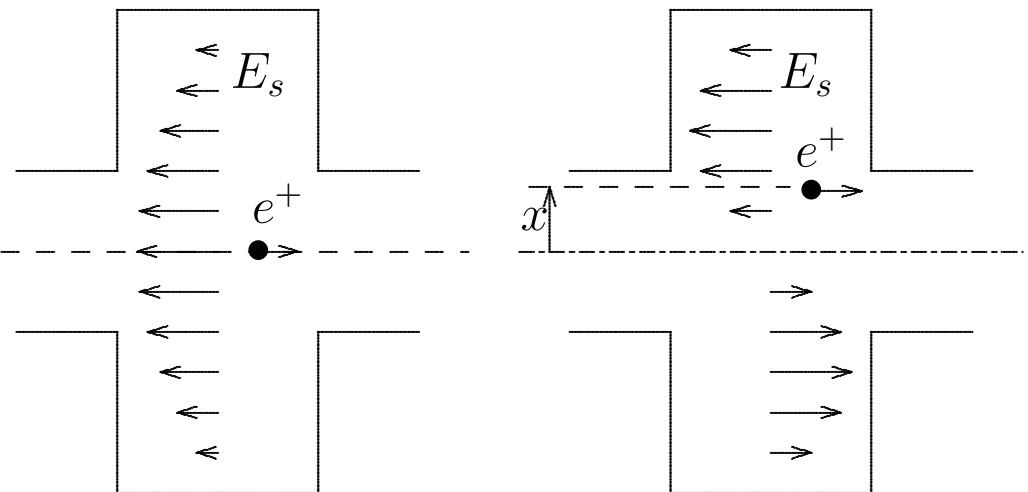


Wall current induced by a bunch

Loop monitor: The magnetic field of the beam induces a voltage in the loop. If the strip forming the loop is of finite width the electric field induces surface charges. The coupling to the beam is inductive for a thin loop and capacitive for a wide one. With the two balanced it is often called 'strip line monitor'.

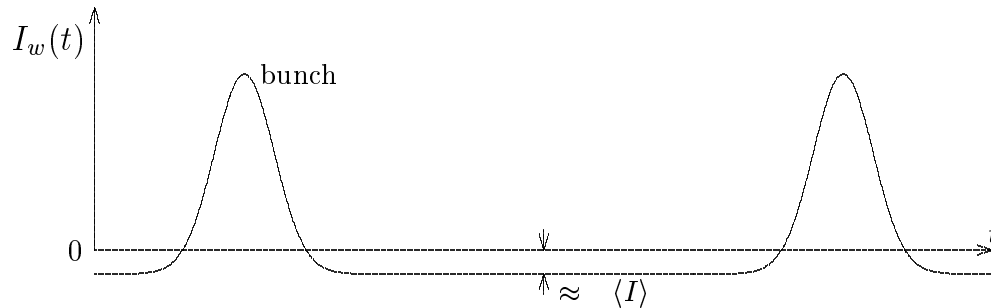


Cavity monitor: Cavity gets excited by multiple bunch passages and oscillates in a monopole (left) as intensity or dipole (right) mode as position monitor. It has a high sensitivity and is used for low intensities.



Measure the average current

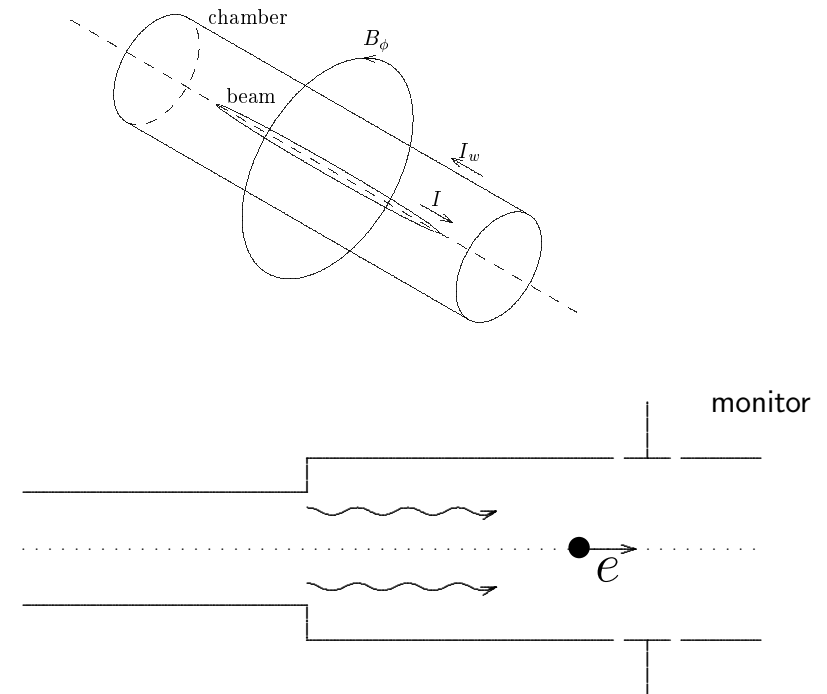
The wall current induced by the beam does not contain the DC-part. However, it can be estimated from the monitor reading between the widely spaced bunches.



Position monitors and radiation field

Diffraction radiation from aperture changes can propagate and reach monitors if above cut-off frequency, $\omega_{\text{cur-off}} \geq 2.405c/a$ with circular chamber radius a . Monitor signals should be low-pass filtered.

Magnetic field created by DC-part of beam does not induce a wall current but penetrates and can be used to measure the average current outside.

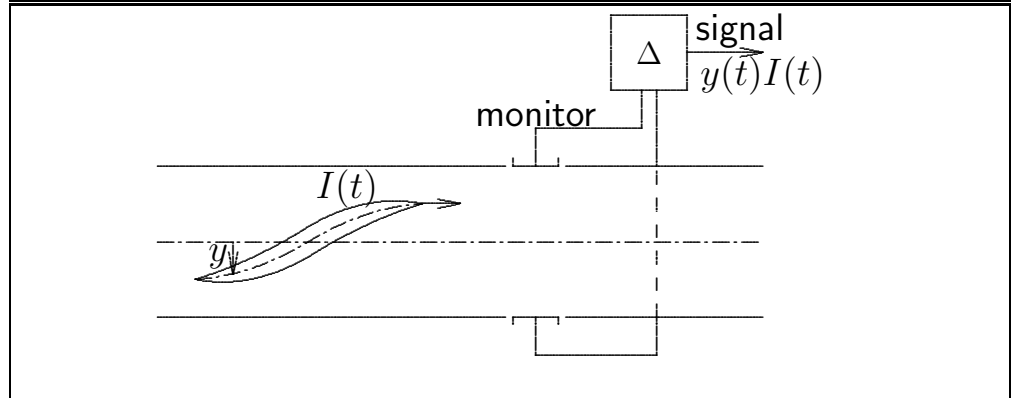
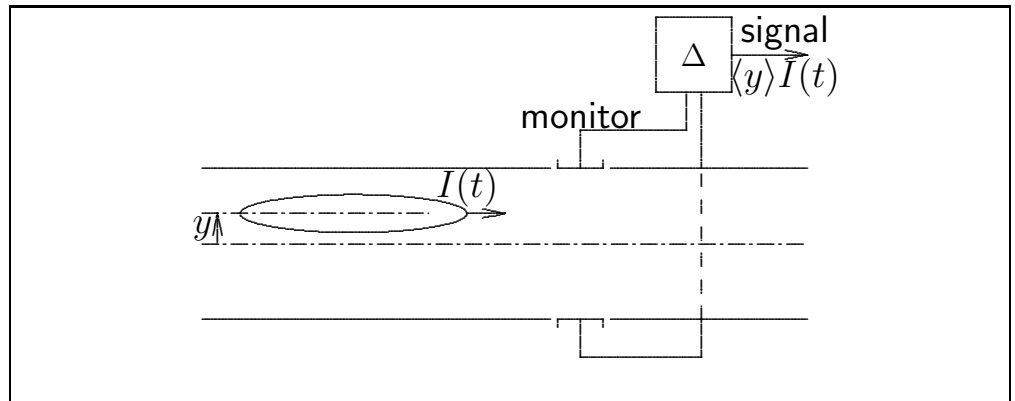
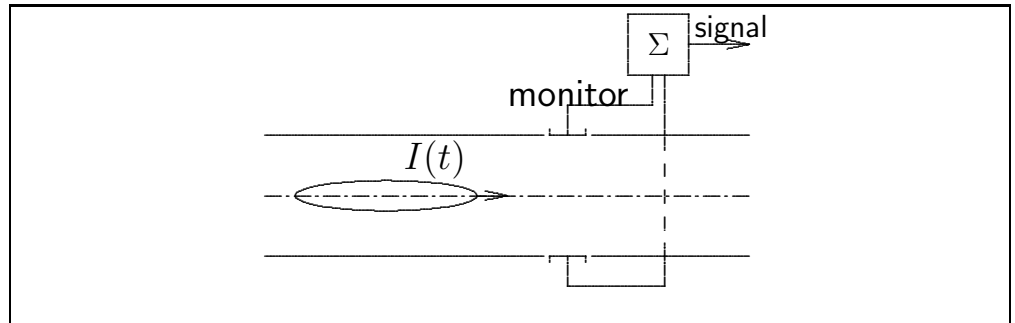


Bandwidth and read-out

Intensity monitors, read-out and signal processor have limited bandwidth. They integrate/differentiate or distort signal. Might only give $I_b = \langle I(t) \rangle$ but over limited bandwidth original signal $I(t)$ may be restored.

A position monitor with low bandwidth measures just the average dipole moment of the bunch $y_b I_b = \langle y(t) I(t) \rangle$.

For larger bandwidth the bunch length can be resolved $y_b I(t)$ and for long bunches of a very large bandwidth also the position variation along the bunch can be observed (head-tail modes).



Fourier transform - spectrum and network analyzers

Fourier Transform converts $f(t) \rightarrow F(\omega)$

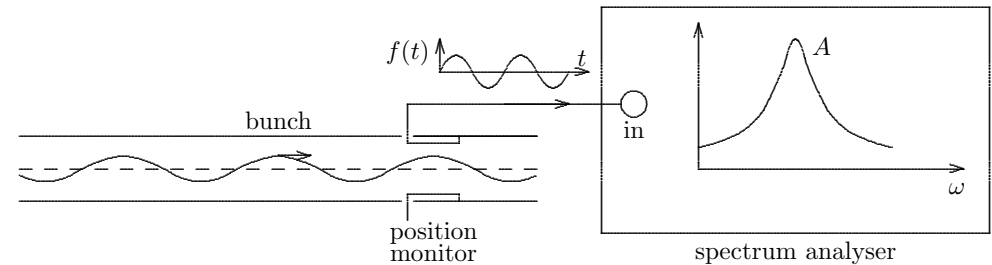
$$\begin{aligned} F(\omega) &= \mathcal{F}[f(t)] = 1/\sqrt{2\pi} \int_{-\infty}^{\infty} f(t)e^{-i\omega t} dt \\ &= \frac{1}{\sqrt{2\pi}} \int f(t) [\cos(\omega t) - i \sin(\omega t)] dt \\ &= F_r(\omega) + iF_i(\omega) \end{aligned}$$

The cosine and sine transforms, called also real and imaginary part or resistive and reactive part, expressed also in amplitude and phase $A^2(\omega) = |F_r(\omega)|^2 + |F_i(\omega)|^2$, $\tan \phi = \frac{F_i(\omega)}{F_r(\omega)}$
 $A^2 \propto$ power spectrum. Inverse transform

$$f(t) = \mathcal{F}^{-1}[F(\omega)] = \frac{1}{\sqrt{2\pi}} \int_{-\infty}^{\infty} F(\omega)e^{i\omega t} dt.$$

Periodic functions are developed in a series

$$\begin{aligned} f(t) &= a_0 + 2 \sum_1^{\infty} (a_p \cos(p\omega_0 t) + b_p \sin(p\omega_0 t)) \\ a_p &= (1/T_0) \int_0^{T_0} f(t) \cos(p\omega_0 t) dt \\ b_p &= (1/T_0) \int_0^{T_0} f(t) \sin(p\omega_0 t) dt. \end{aligned}$$

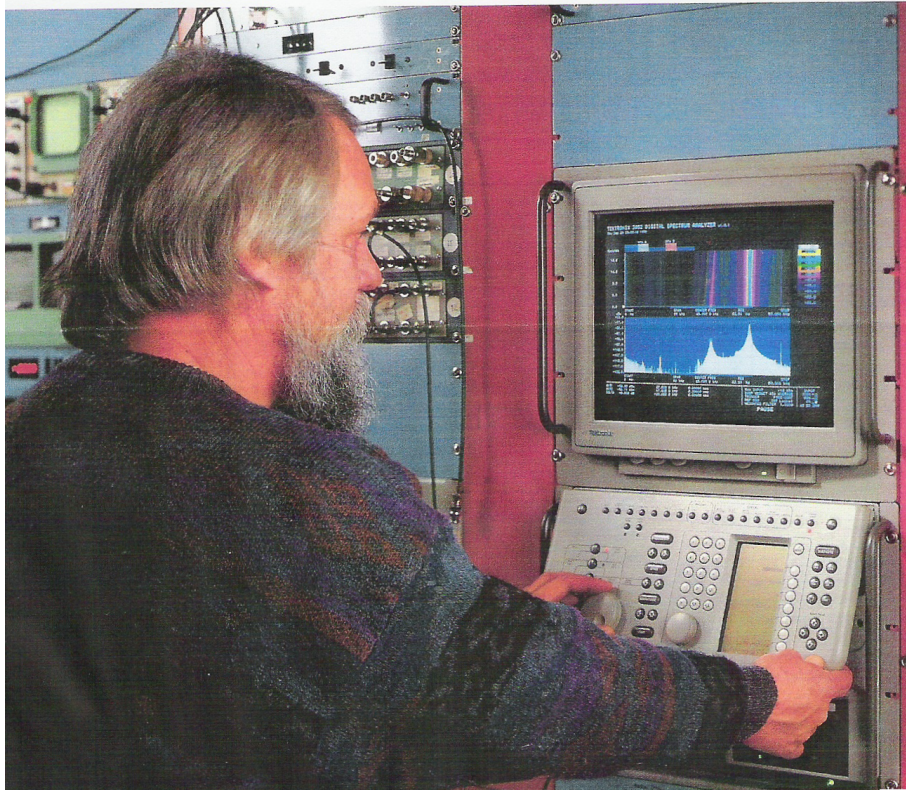


Spectrum analyzer Fourier transforms time signal $f(t)$ but integration range is limited and only amplitude is obtained, no phase since no absolute time involved. Most analyzers use swept frequency, i.e. at any moment only one frequency with finite bandwidth $\delta\omega$ is measured. Sweep speed is limited by the desired band-width. Some spectrum analyzers store signal $f(t)$ over certain time span make a Fast Fourier Transform (FFT) while the next time sample and a certain spectral range of interest is observed all the time.

Advanced analyzer — Digital Signal Processing, CAS 2007

Real time analyzer with parallel processor have been developed for RADAR

3052 DSP SYSTEM AT SLAC

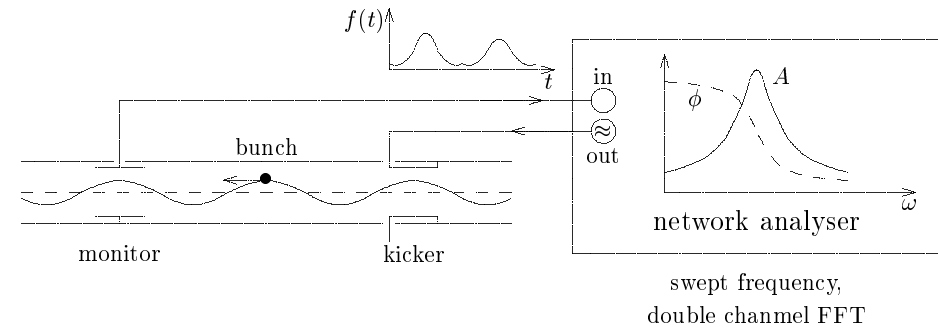


Search for **E**xtra **T**errestrial **I**ntelligence
Unknown frequency, modulation, communication method, etc.

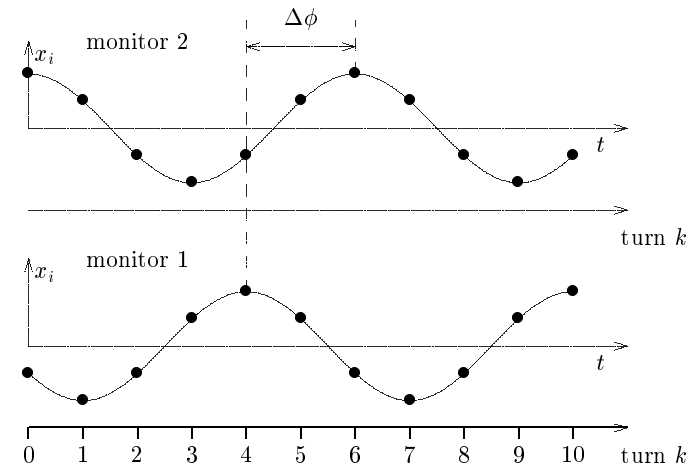


Network analyzer

A Network analyzer measures the beam response in amplitude A and phase ϕ , or in real $F_r(\omega)$ and imaginary $F_i(\omega)$ part, to harmonic excitation, **transfer function**. Most use a swept frequency, some a double channel FFT analyzer and noise excitation.



We can also compare relative amplitude and phase response of two monitors to a beam excitation and get information about beta function and phase.

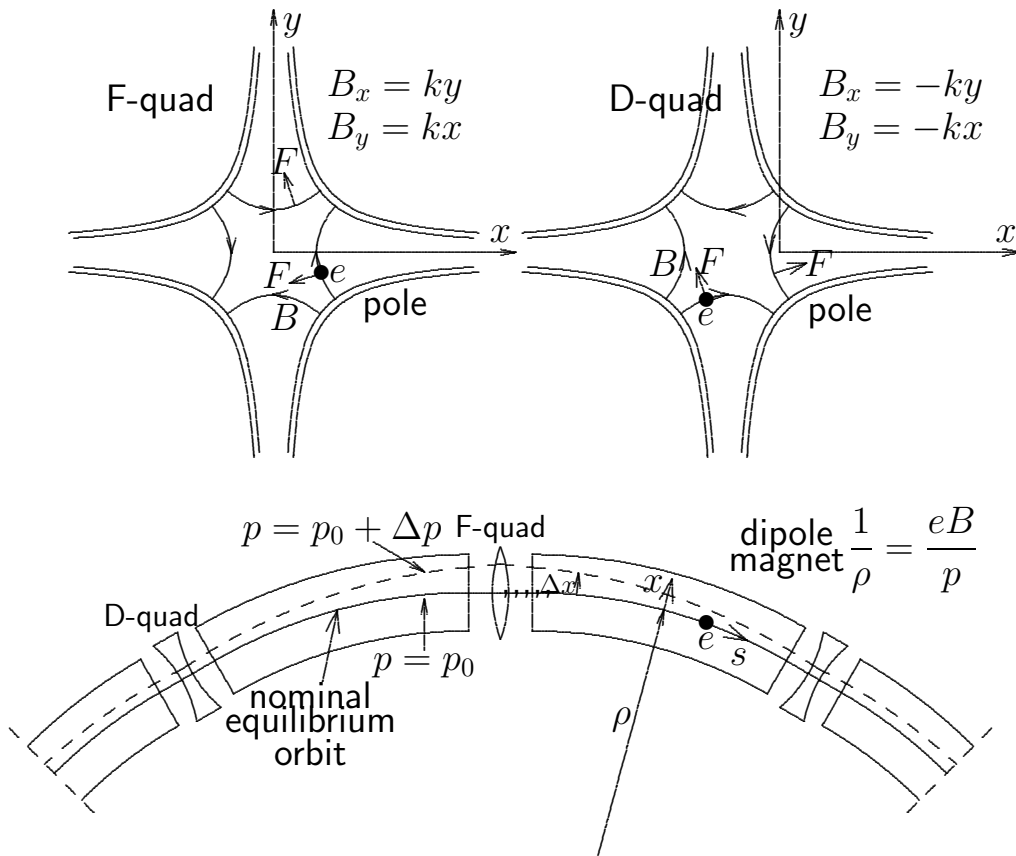


2) TRANSVERSE EFFECTS

Measurements

instruments conditions	position monitor	deflector, change ring parameters
static, equilibrium conditions	closed orbit, lattice functions, phys. aperture	orbit correction bumps
dynamic, oscillations, turn by turn	tunes, lattice functions, dyn. aperture	excite transverse oscillations
excitation-response relation	pulse excitation: Green function harmonic excitation: transfer function	

Ring elements and dynamics



Storage ring has bending dipole and focusing quadrupole magnets, arranged in lattice, equilibrium orbit for nominal position, angle, momentum p_0 , revolution frequency ω_0 .

Field gradients of quadrupoles focus horizontally in F, vertically in D-quad, quantified by $K = (e/p)(dB_y/dx) = d(1/\rho)/dx$ with $\ell K = 1/f$.

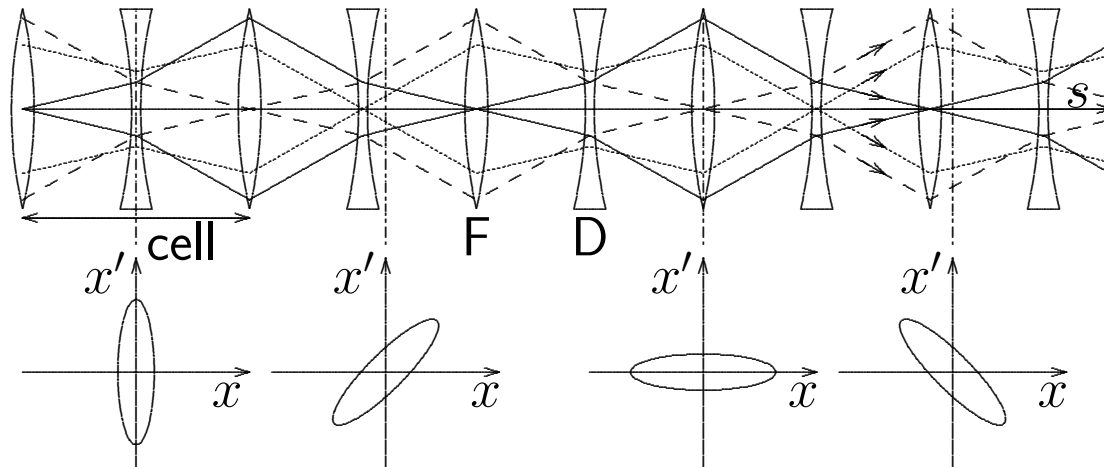
Deviations x/y and x'/y' from nominal are focused, betatron oscillations around orbit. Their maximum amplitude is a measure for local focusing strength, given by so-called beta functions $\beta_{x/y}$. Number of oscillations per revolution $Q_{x/y}$, called tunes, measure global focusing strength.

Particle with momentum deviation Δp , bent differently by dipoles, different orbit, displaced $\Delta x = D_x \Delta p / p_0$ (D =dispersion), circumference C_0 , revolution frequency ω_0

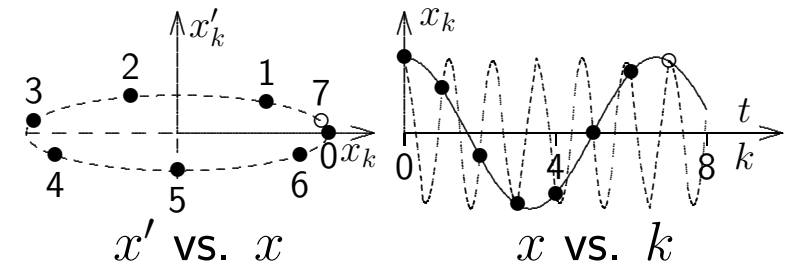
$$\frac{\Delta C}{C_0} = \alpha_c \frac{\Delta p}{p}, \quad \frac{\Delta \omega_0}{\omega_0} = \eta_c \frac{\Delta p}{p_0}, \quad \eta_c = \alpha_c - \frac{1}{\gamma^2}$$

α_c =momentum compaction, computed.

Single particle trajectory observed turn by turn

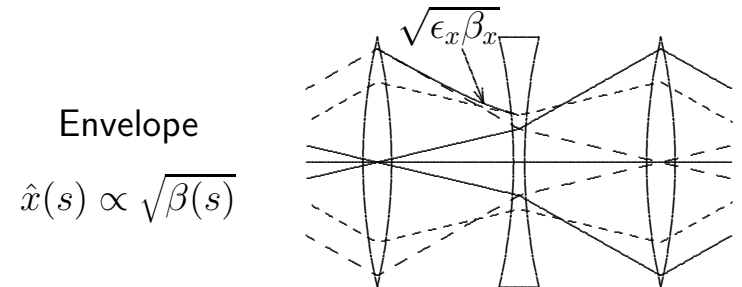


In storage ring with linear focusing by F and D-quads observe position, angle x_k, x'_k at location s of **single particle** each turn k . Plotting x'_k vs x_k gives phase-space ellipse having everywhere same area and emittance $A = \pi\epsilon$ but different shape. In F-quad x_k are large but angles x'_k small giving low, flat ellipse, in D-quads high and narrow ellipse. Their heights and widths are maxima \hat{x}' and \hat{x} in many turns, product gives $\epsilon_x = \hat{x}'\hat{x} = \text{const.}$, ratio $\beta(s) = \hat{x}/\hat{x}'$. Between quads, ellipses tilted, x'_k/x_k -correlation < 0 after F, > 0 after D-quad, complicated $\epsilon, \beta(s)$ expression.



Trajectory represents betatron oscillation, with number $Q/\text{turn} = \text{tune}$. Not harmonic in s , but expressed by computed $\beta(s)$, phase $\phi(s)$

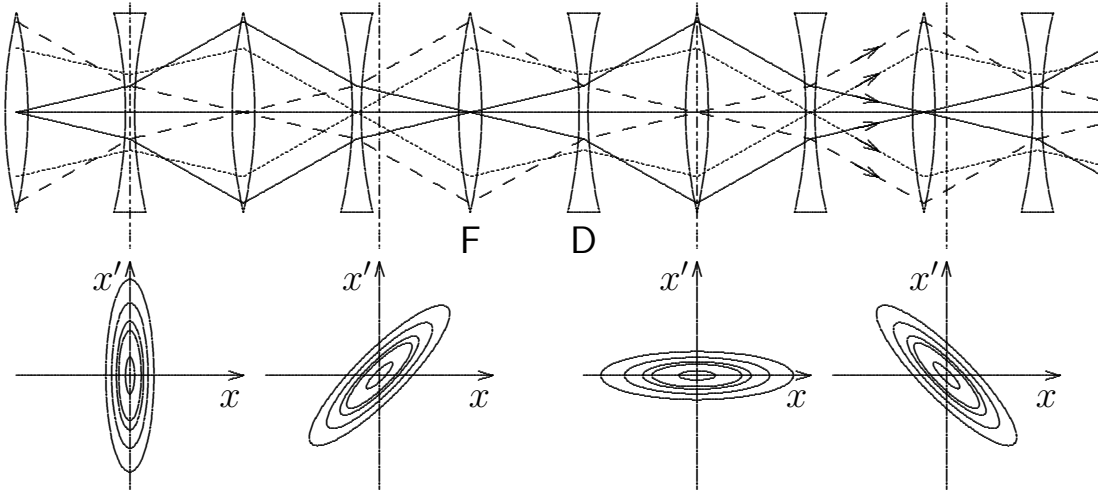
$$x(s) = \sqrt{\epsilon\beta(s)} \cos(\phi(s) - \phi_0)$$



Points x_k at fixed location s plotted against k can be fitted with harmonic functions $\sin((p \pm q)\omega_0 t)$, fractional tune $q = Q - \text{integer}$, revolution frequency ω_0 .

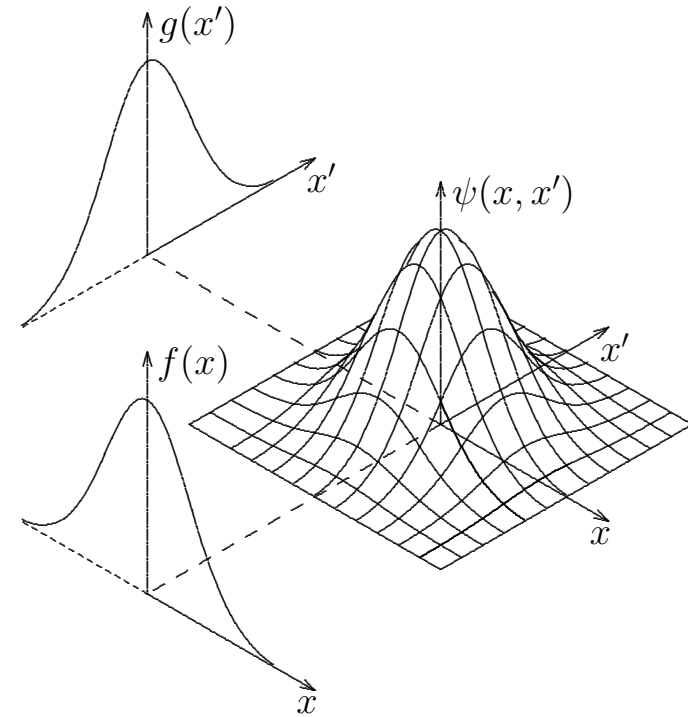
Many particles — distribution

Many particles oscillating with different phase, amplitude, emittance ϵ_i but same ratio $\hat{x}_i/\hat{x}' = \beta_x$. Distribution of emittances with average $\epsilon = \langle \epsilon_i \rangle$



The phase space distribution $\psi(x, x')$ is not measured directly but its projected spatial $f(x)$ and angular $g(x')$ distributions with center-of-mass, variances or RMS values.

$$f(x) = \int \psi(x, x') dx', \quad g(x') = \int \psi(x, x') dx$$

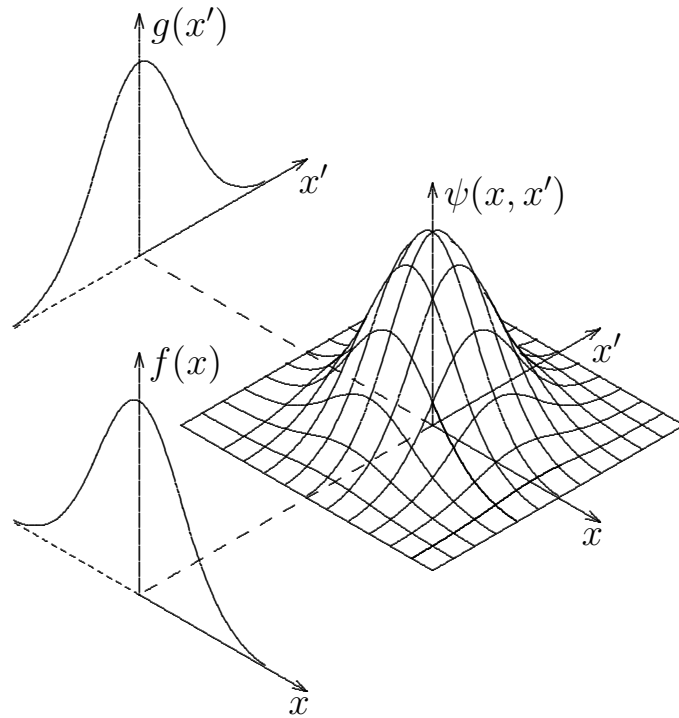


$$\langle x \rangle = \frac{\int f(x) x dx}{\int f(x) dx}, \quad \langle x' \rangle = \frac{\int g(x') x' dx'}{\int g(x') dx'}$$

$$\sigma_x^2 = \frac{\int f(x) x^2 dx}{\int f(x) dx}, \quad \sigma_{x'}^2 = \frac{\int g(x') x'^2 dx'}{\int g(x') dx'}$$

$$\epsilon_x = \langle \epsilon_x \rangle \approx \sigma_x \sigma_{x'}$$

Distribution measurements



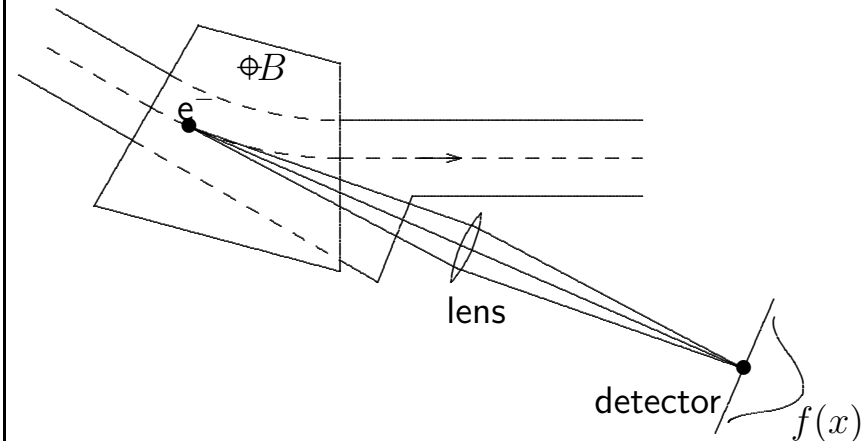
$$f(x) = \int \psi(x, x') dx', \quad g(x') = \int \psi(x, x') dx$$

With beam position monitors

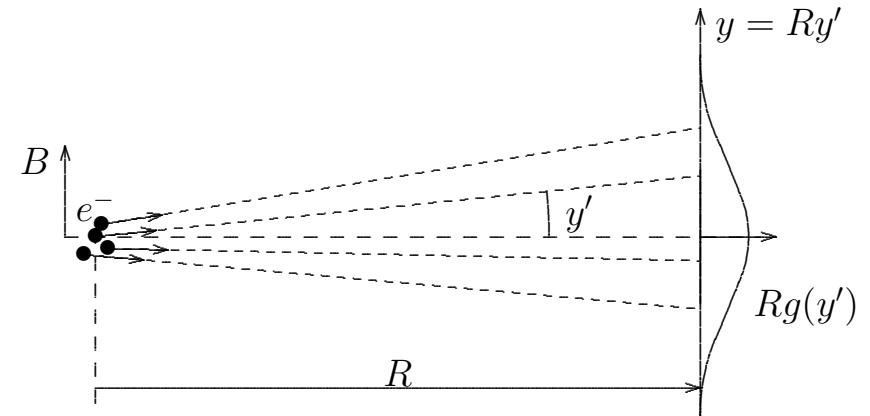
Center-of-mass position $\langle x \rangle$, with a close pair of monitors also center-of-mass angle $\langle x' \rangle$.

In measurements of whole beam the center-of-mass behaves like a single particle.

Imaging with SR $\rightarrow f(x)$ and σ_x



Direct SR observation $\rightarrow g(x')$ and σ'_x

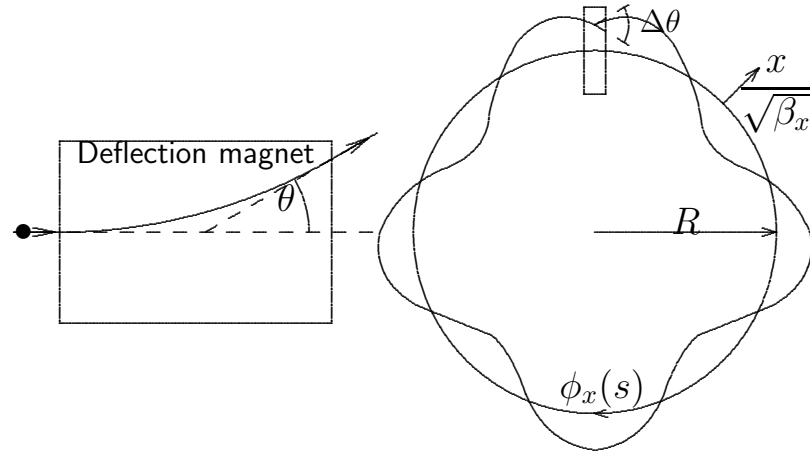


Emittance

$$\epsilon = \frac{\langle x^2 \rangle}{\beta_x} = \frac{\sigma_x^2}{\beta_x} \approx \sigma_x \sigma'_x$$

Closed orbit perturbation by a dipole

With a short dipole magnet we make a deflection $\Delta\theta$ and calculate the new closed orbit.



$$x(s) = \sqrt{\epsilon\beta(s)} \cos(\phi(s) - \phi_0)$$

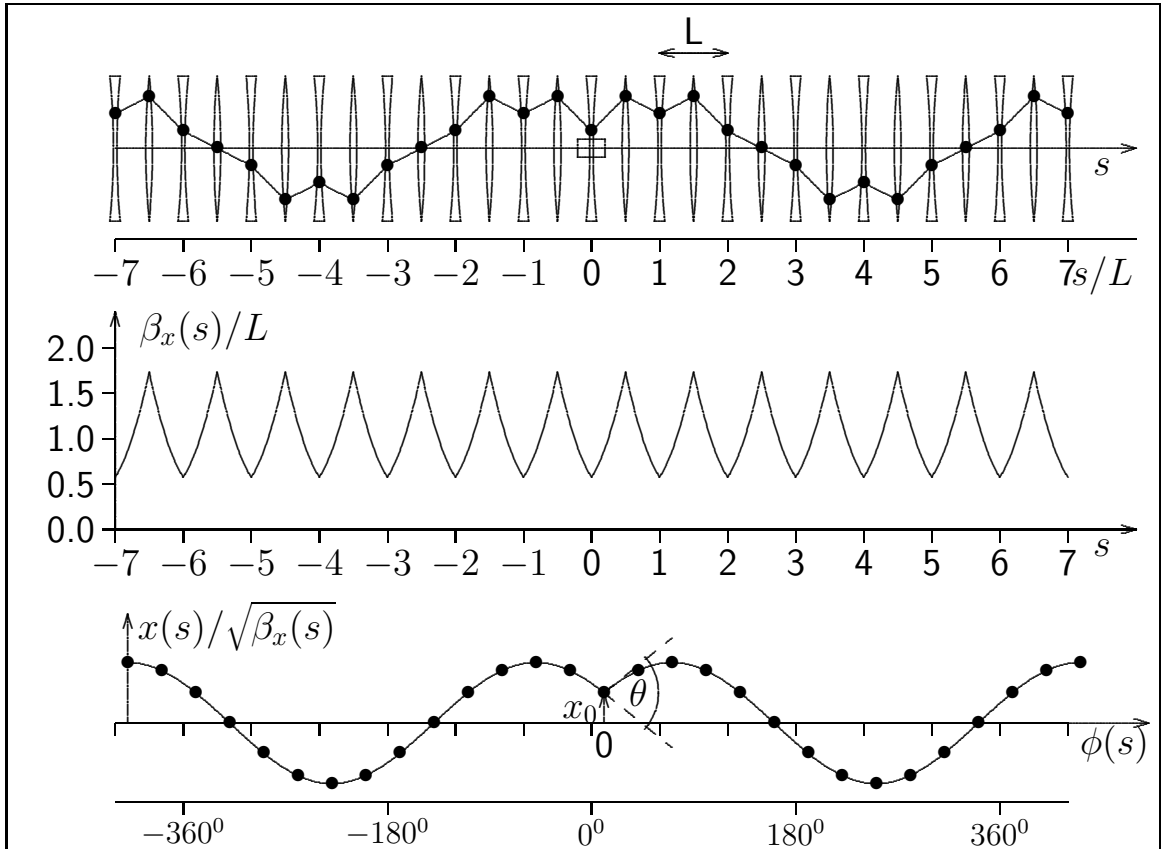
$$x(0) = x(2\pi R)$$

$$x'(0) = x'(2\pi R) + \Delta\theta$$

$$x(0) = \frac{\Delta\theta\beta_x(0)\cos(\pi Q)}{2\sin(\pi Q)}$$

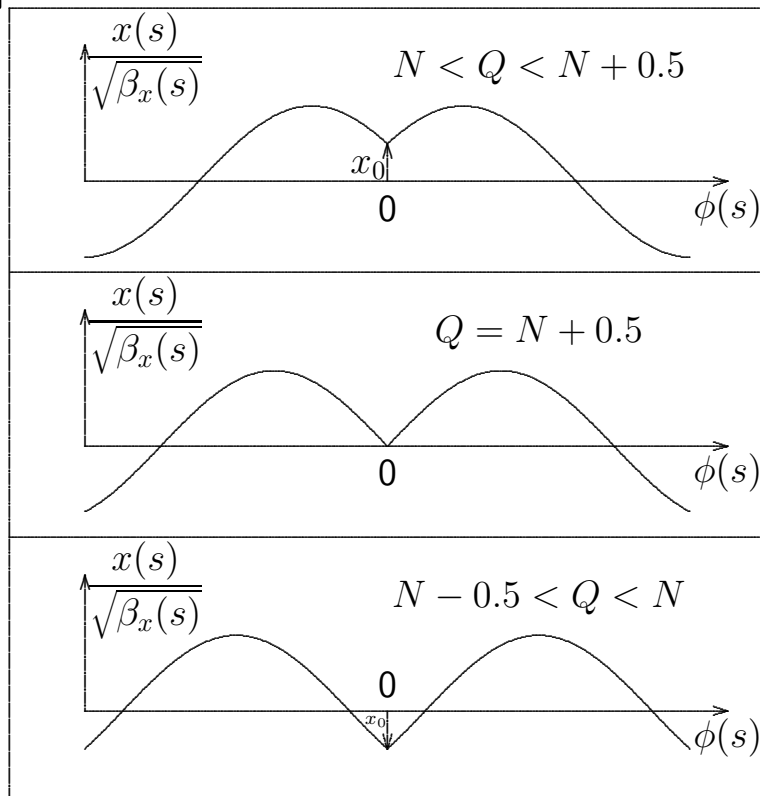
$$Q = \phi(2\pi R) - \phi(0) = \text{tune}$$

If Q is close to integer the distortion is large - integer stop band.



Raw measurement of distorted orbit (top) is scaled with root of beta function (middle) and plotted against phase advance ϕ (bottom). Optics check, deflection, measure orbit distortion, compare with calculated $\beta(s)$ and $\phi(s)$. Phase separation of two points by $n\pi$ changes only if error is in between.

Cusp of distortion for different tunes

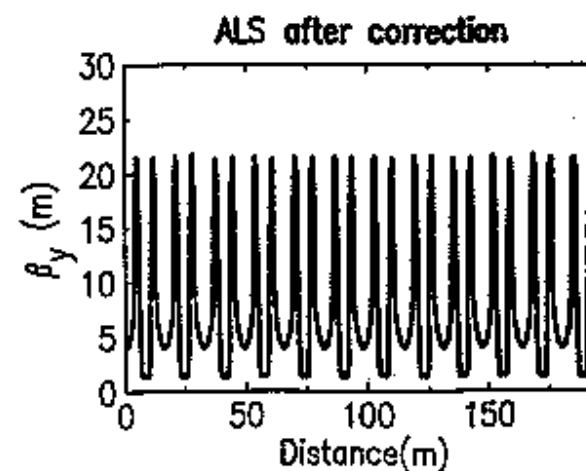
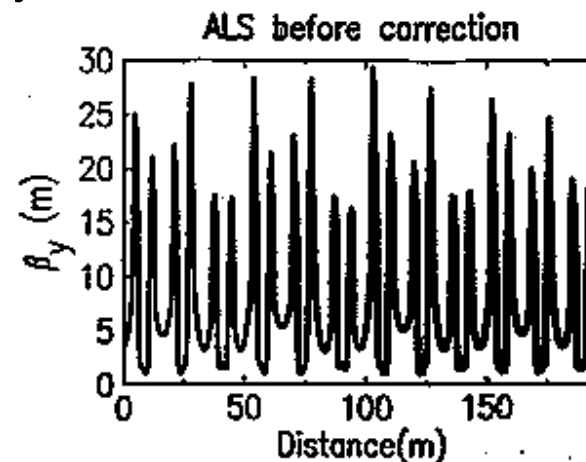


Qualitative cusp tells if tune is above or below half integer, quantitative x_0 gives either Q or $\beta(0)$, not accurate, needs minimal instrumentation, works in presence of noise and coupling, likes monitor and deflector close by.

$$x_0 = \frac{\Delta\theta\beta(0)\cos(\pi Q)}{2\sin(\pi Q)}.$$

Response matrix

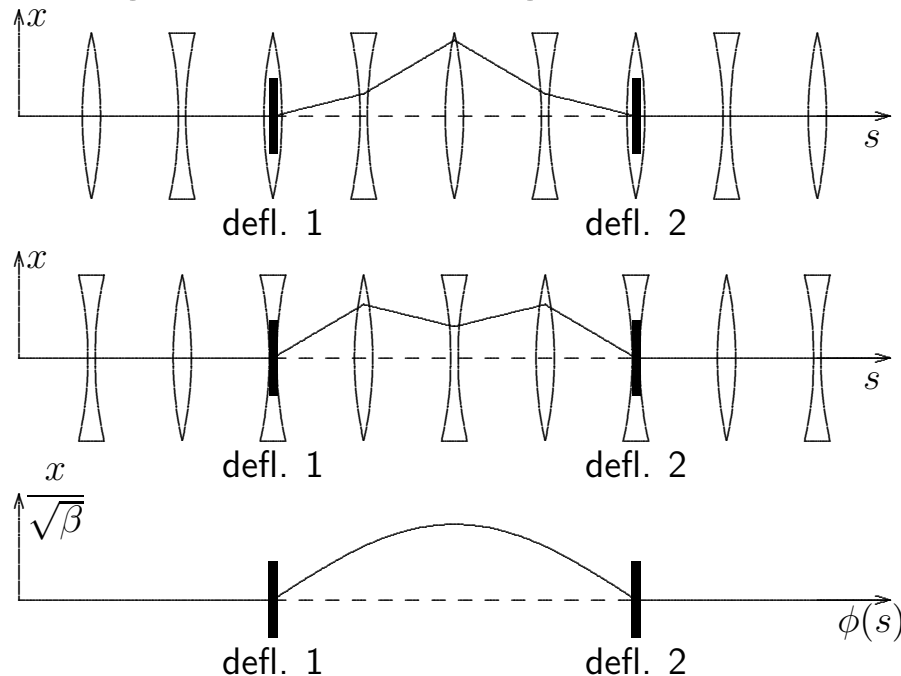
Many correctors and monitors give 'response matrix' and measures beta function at many locations and check calibrations.



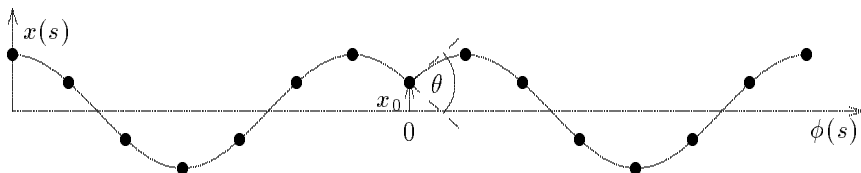
ALS: Robin, Safranek, Portmann, Nishimura

Beam bumps

Few correctors are powered to make local bump without effect outside. To probe physical aperture, scrape beam tails, centering special magnets, find coupling sources, etc.



Orbit correction



Most important for position monitors and correctors is closed orbit measurement and correction. Based on figure about 2 monitors/correctors per betatron wavelength are needed and at strategic points, interaction region, undulators, a few more including a pair without magnets in between. Different strategies are used, global correction based on orbit harmonics, local one with beam-bumps, find most effective corrector and many more. Ideal orbit goes through quadrupole centers. Check monitor alignment by observing beam position or tune motion vs. quadrupole or sextupole strength, 'beam based alignment'.

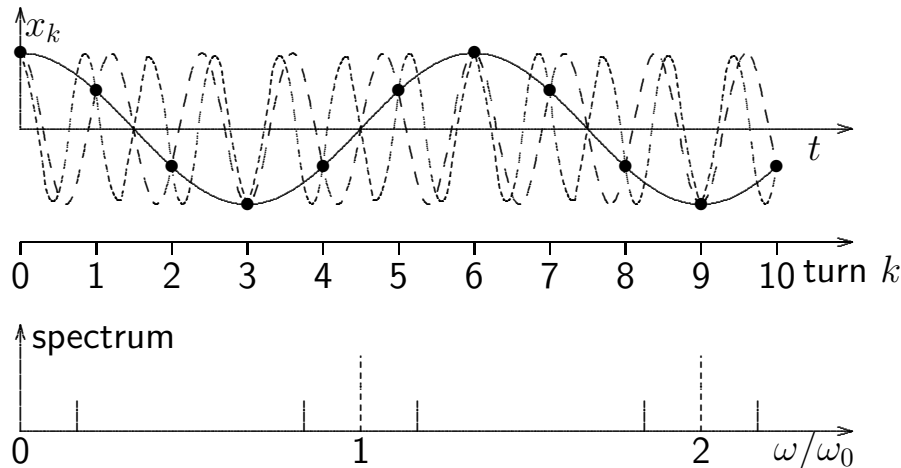
$$\Delta x' = -x_o/f = -x_0 L \Delta K,$$

with K = quad strength parameter.

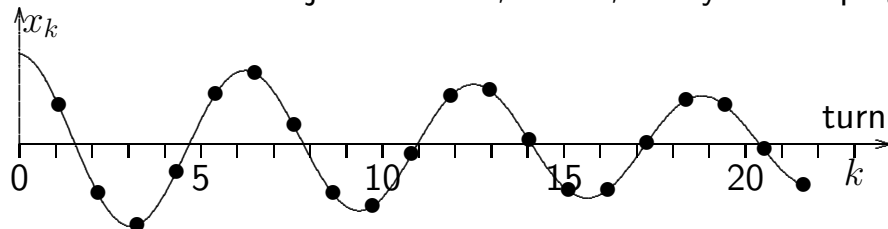
Measuring betatron frequency — tune

Oscillating bunch in time and frequency.

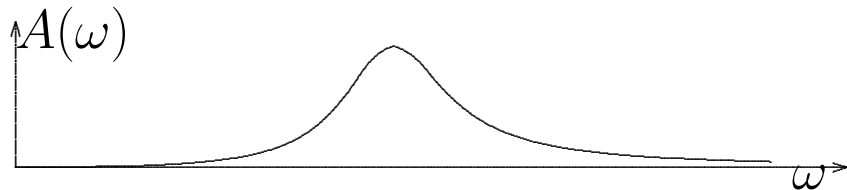
$$x_k = \hat{x} \cos(2\pi qk), \quad \omega_\beta = (p \pm q)\omega_0, \quad q = \frac{1}{6}$$



Pulse excitation: injection error, kicker, decay = damping

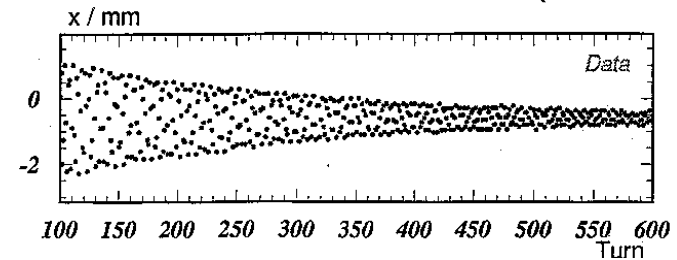


Harmonic excitation: swept frequency, width=damping

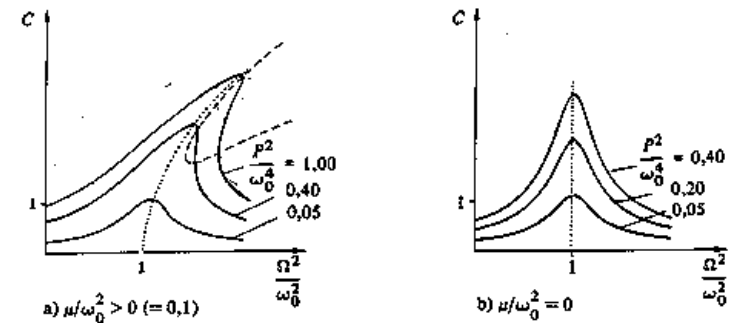


Green function, transfer function;
equivalent, but non-linearities.

Pulse excite fit vs. amplitude (A. Müller)



Harmonic excitation, sweep both ways



Applications:

Measure ω_β fractional tune q , test optics.

$q = q(\Delta K)$ tune vs. quad, β

Dynamic aperture

Vertical kick, horizontal response

$q = q(\Delta E) \rightarrow Q'$ chromaticity

Measuring β -function at a quadrupole

Variation $L\Delta K = \Delta(1/f)$ of single quadrupole changes tune ΔQ proportional to local β which offers an important optics check

$$\Delta Q = \frac{\beta}{4\pi} L \Delta K \rightarrow \beta = \frac{4\pi}{L} \frac{\Delta Q}{\Delta K}.$$

This assumes **small** ΔQ otherwise β itself changes giving quadratic expression in ΔQ

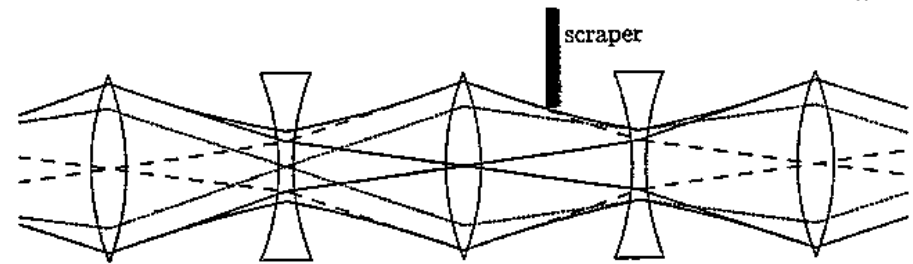
$$\beta = \frac{4\pi}{L} \frac{\Delta Q}{\Delta K} \left(1 + \frac{\Delta Q}{\tan Q} \right).$$

Still short lens approximation, longer quadrupole involve neighborhood optics. Best simulate quadrupole change on computer code and compare.

Hysteresis makes $\Delta K/K \neq \Delta I/I$ and limit accuracy demanding small changes or recycling. Incorporate a loop in quad and measure induced integrated voltage to get directly the flux change.

Measure dynamic acceptance

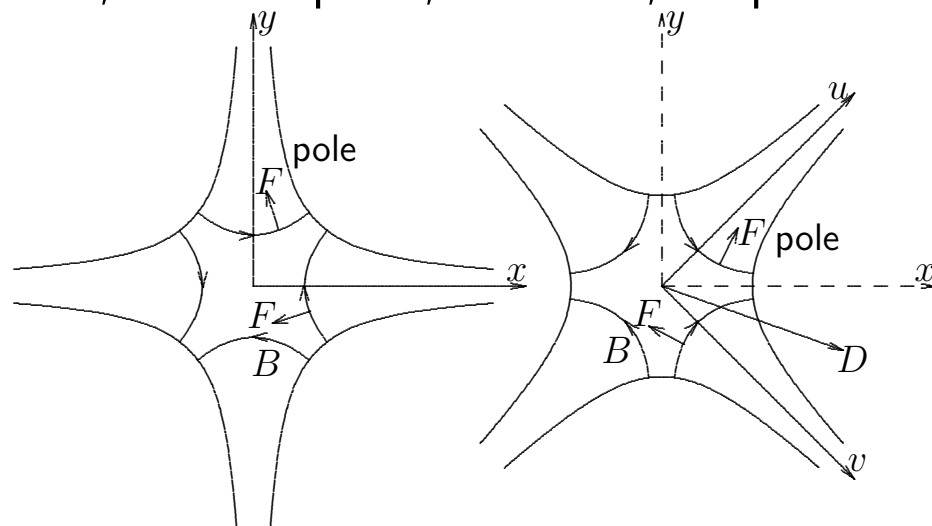
Dynamic acceptance gives normalized maximum betatron oscillation amplitude of beam optics, i.e. the maximum beam emittance. Limited by non-linear elements giving tune changes with amplitudes making oscillations unstable. Measured by exciting oscillation and increasing amplitude until life-time is short. To calibrate, scraper is moved into beam to a distance x_a where gets even shorter, acceptance $A = x_a^2/\beta$.



At life-time limit check tune in case of resonances. To avoid orbit distortion effects move scraper from both sides, window scraper.

Coupling measurement

Horizontal and vertical betatron oscillations are usually treated as independent. Some elements, rotated quads, solenoids, couple them



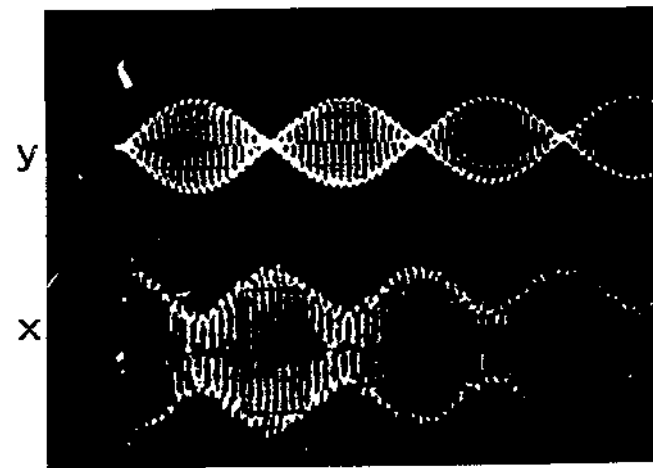
normal quadrupole

rotated quadrupole

$$\ddot{x} + Q_x^2 \omega_0^2 x = ky, \quad \ddot{y} + Q_y^2 \omega_0^2 y = kx$$

Excitation response in both planes

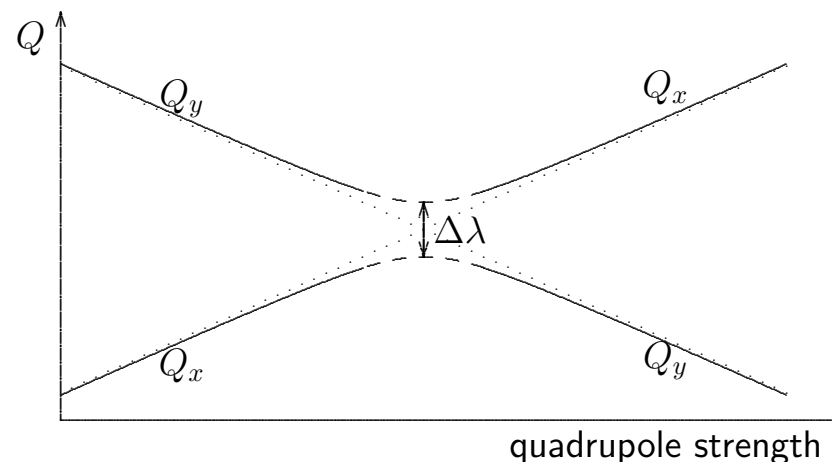
Takinawa, ISR: Beam is excited horizontally, response in this plane (bottom) and vertical (top) are shown. Energy is exchanged, same modulation in both planes if $\beta_x \approx \beta_y$.



Closest tune approach:

Increasing F-quad approaches tunes to minimum value $\Delta\lambda$ and separate them again

$$\Delta\lambda \approx k/(Q\omega_0)$$

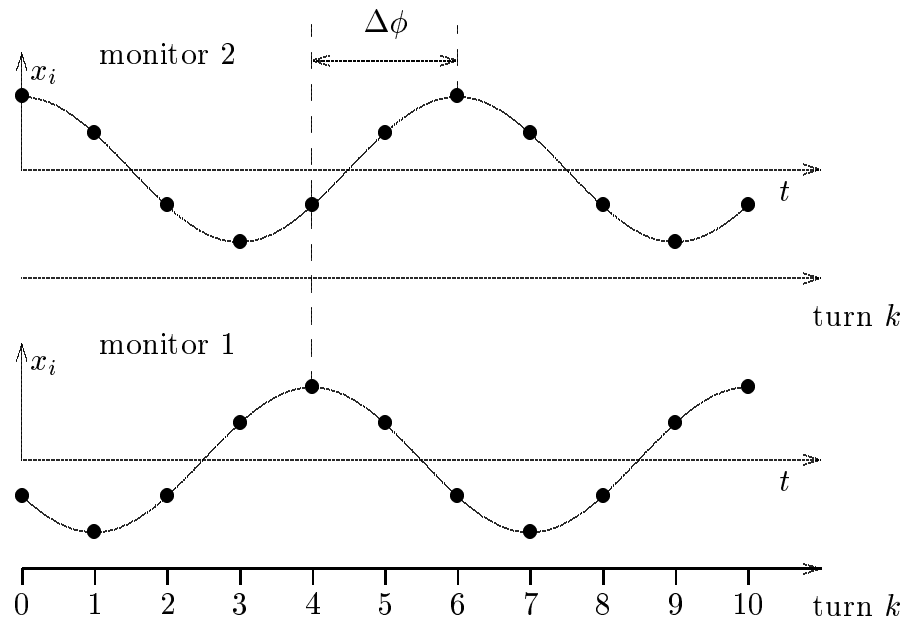


Beta function and phase advance

An excited oscillation is measured in monitors i each revolution k

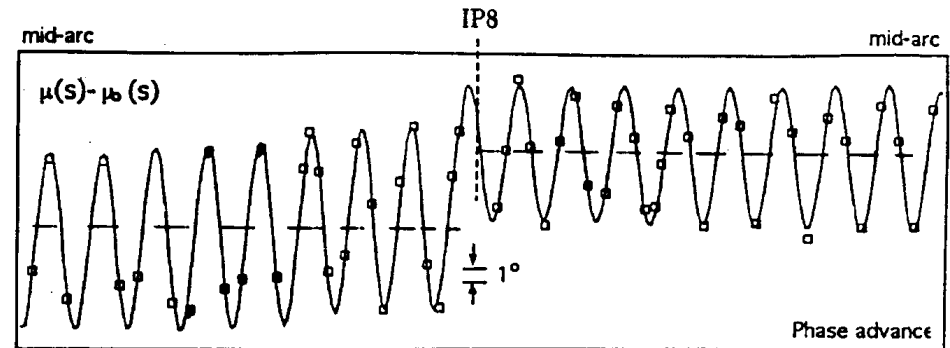
$$x_{ik} = \frac{\hat{x}}{\sqrt{\beta_{x0}}} \sqrt{\beta_{xi}} \cos(2\pi Q_x k + \mu_{xi})$$

get β_{xi} , μ_{xi} phase advance $\Delta\phi = \mu_{i+1} - \mu_i$, has small systematic errors, bunch signal gives cable delays. $\beta_{x,i+1}/\beta_{x,i} = (\hat{x}_{i+1,k}/\hat{x}_{i,k})^2$ needs calibration.



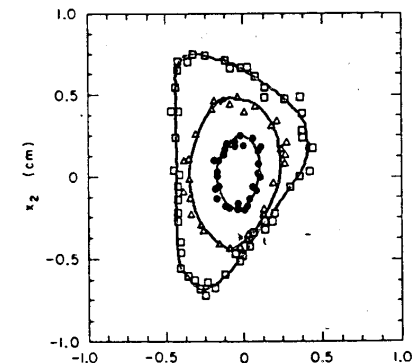
Check optics by phase measurement

Measuring betatron phase around ring and comparing calculation we check beam optics and locate errors. Local focusing error creates a $\beta(s)$ beating around the ring at twice the betatron frequency, i.e. points being separated by $n\pi$ will keep this separation unless the error is located in between them.



Beta beating caused by a focusing error

Experimental tracking to check a simulation, P. Morton et al.



3) LONGITUDINAL EFFECTS

Measurements

instruments conditions	position monitor fast intensity monitors	RF-modulation, change ring parameters
static, equilibrium conditions	mom. compaction, bunch length, energy aperture	adjust RF-frequency, energy
dynamic, oscillations, turn by turn	synchrotron tunes, dispersion, dynamic energy aperture	excite longitudinal oscillations
excitation-response relation	harmonic excitation: longitudinal transfer function	

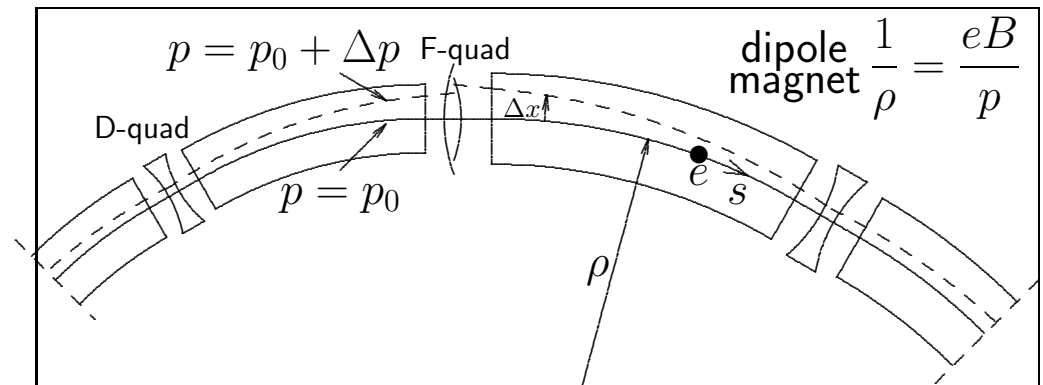
Longitudinal dynamics

Particle $\Delta p > 0$ is bent less in dipoles, its closed orbit is outside from nominal by $\Delta x(s)$ and gets extra bending in quadupoles. Circumference of this off-momentum orbit is changed by ΔC . In linear approximation

$$\Delta x = D_x \frac{\Delta p}{p_0}, \quad \frac{\Delta C}{C_0} = \alpha_c \frac{\Delta p}{p_0}, \quad \alpha_c = \left\langle \frac{D_x(s)}{C_0 \rho} \right\rangle.$$

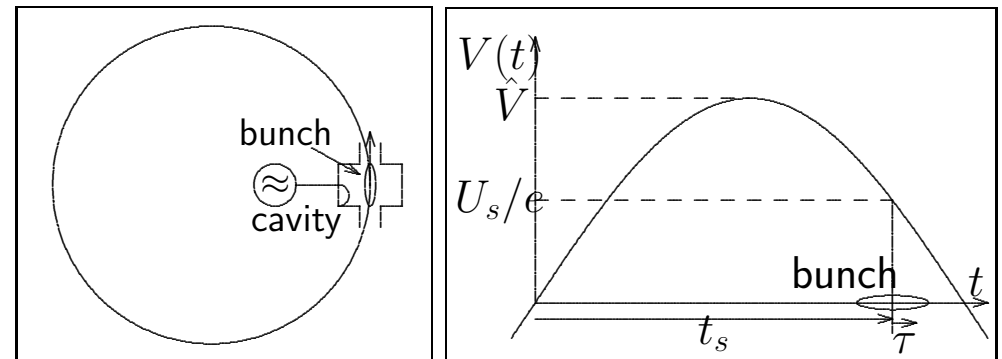
D_x and α_c , are computed with optics codes. Different C and β_C of off-momentum particles change revolution time T , frequency ω_0

A cavity is oscillating with peak voltage \hat{V} at frequency $\omega_{RF} = h\omega_r$, being a harmonic h of the nominal revolution frequency, replaces the energy U_s lost per particle and turn and provides energy focusing.



$$\frac{\Delta T}{T_0} = -\frac{\Delta \omega_0}{\omega_0} = \left(\alpha_c - \frac{1}{\gamma^2} \right) \frac{\Delta p}{p_0} = \eta_c \frac{\Delta p}{p_0}.$$

Usually $\alpha_x > 0$, however η_c vanishes at transition energy defined by $\gamma_T^2 = 1/\alpha_c$ and is positive above and negative below this.



RF-system —longitudinal focusing

nominal: $p_0 \approx E_0/c$, $T_0 = 2\pi/\omega_0$

synchr.: t_s , $\phi_s = h\omega_0 t_s$, $e\hat{V} \sin \phi_s = U_s$

deviation: $\tau = t - t_s$, $\Delta E = E - E_0 \ll E_0$

$$\text{dynamics: } \frac{\Delta\tau}{T_0} = -\frac{\Delta\omega_0}{\omega_0} = \eta_c \frac{\Delta p}{p_0}$$

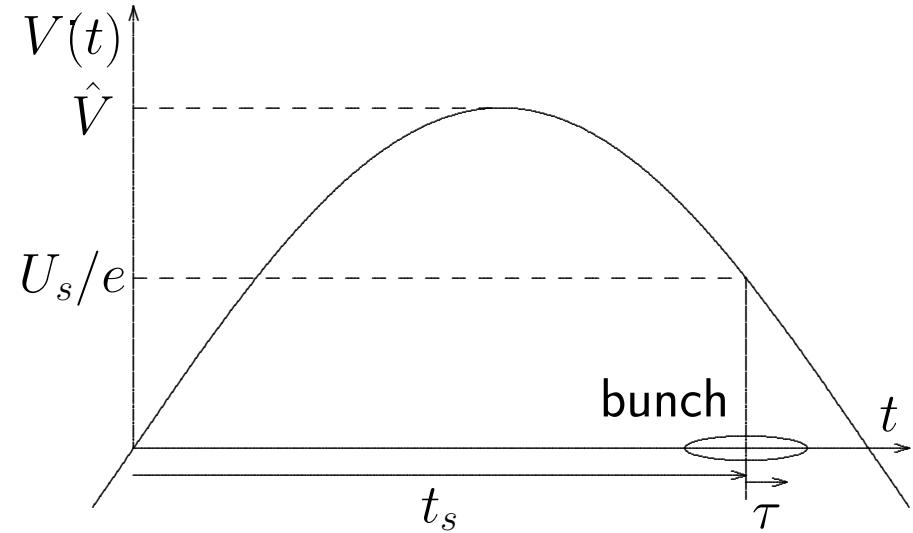
Particle arriving at t_s , $\tau = 0$ receives energy U_s just compensate loss by S.R.

Late particle, $\tau > 0$, gets less voltage, its energy will be lower, goes around faster, arrives earlier next turn and gains more energy. Result, particle oscillates around t_s and E_0 with frequency ω_s , making synchrotron oscillation.

$$\tau = \hat{\tau} \sin(\omega_s t), \quad \epsilon = \hat{\epsilon} \cos(\omega_s t), \quad \hat{\tau} = \eta_c \hat{\epsilon} / \omega_s$$

$$\omega_s^2 = -\omega_0^2 \frac{\eta_c h e \hat{V} \cos \phi_s}{2\pi E_0}, \quad Q_s = \frac{\omega_s}{\omega_0}, \quad \epsilon = \frac{\Delta E}{E}$$

$$\frac{\eta_c \epsilon^2}{2} + \frac{\omega_s^2 \tau^2}{2\eta_c} = \text{Hamiltonian} = \text{const.}$$

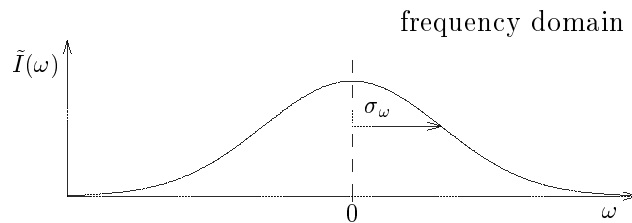
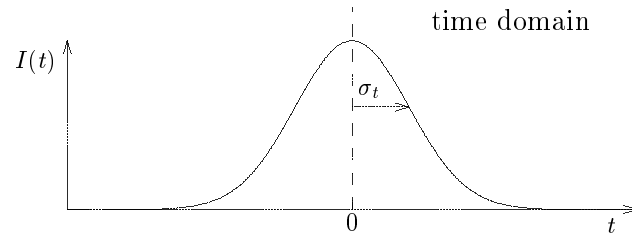


RF-system replaces in average energy lost by synchrotron radiation and focuses in time and energy. Particles oscillate with ω_s around t_s and E_0 and form bunches with distribution in energy and time of RMS values σ_τ and $\sigma_\epsilon = \sigma_E/E_0$

$$\sigma_\tau = \frac{\eta_c}{\omega_s} \sigma_\epsilon = \frac{1}{\omega_0} \sqrt{\frac{2\pi E_0 \eta_c}{h e \hat{V} \cos \phi_s}} \sigma_\epsilon$$

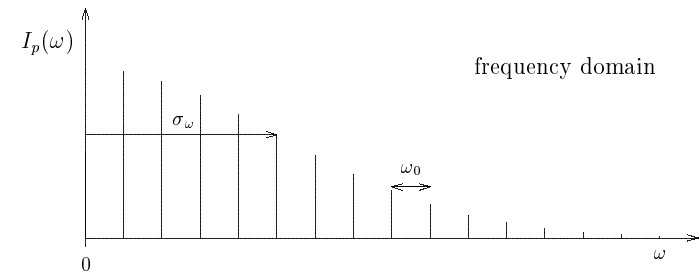
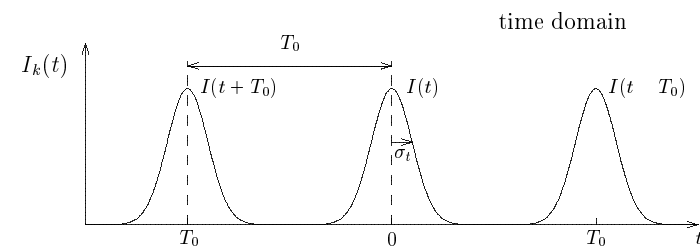
Bunch signals

Measure bunch length and filling pattern.



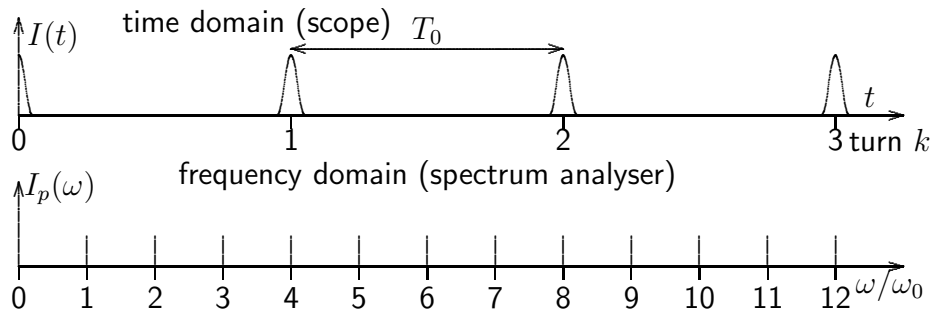
1 bunch single traversal, $\sigma_t \sigma_\omega = 1$

$$\tilde{I}(\omega) = \frac{1}{\sqrt{2\pi}} \int_{-\infty}^{\infty} I(t) \cos(\omega t) dt \quad (\text{symmetric})$$

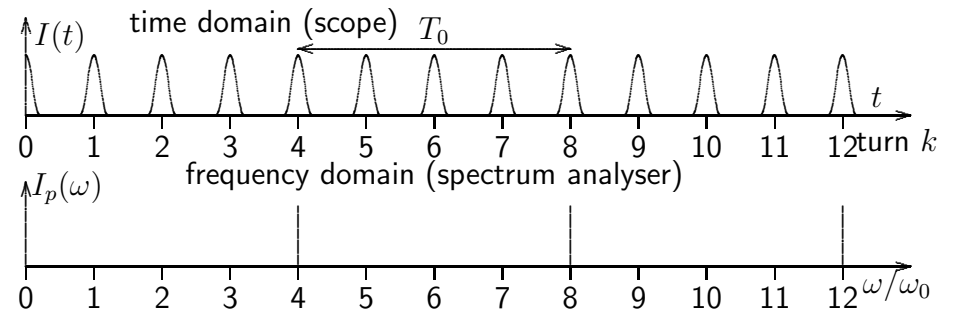


1 bunch multi traversal

$$I_p = \frac{1}{T_0} \int_0^{T_0} I(t) \cos(p\omega_0 t) dt = \frac{\omega_0}{\sqrt{2\pi}} \tilde{I}(p\omega_0)$$

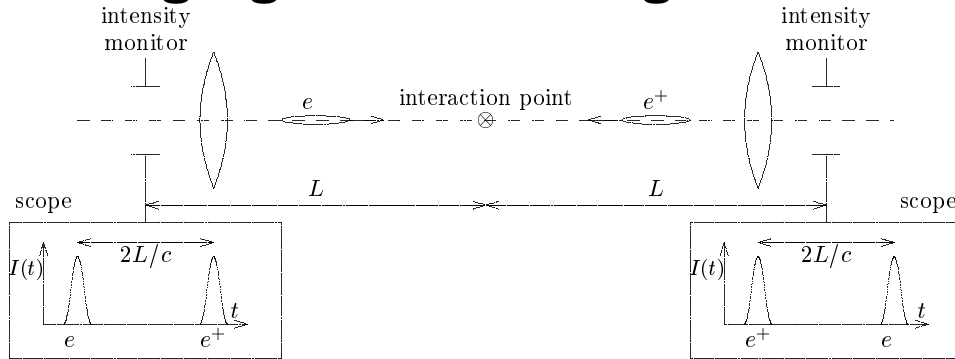


Time/frequency signal of 1 bunches



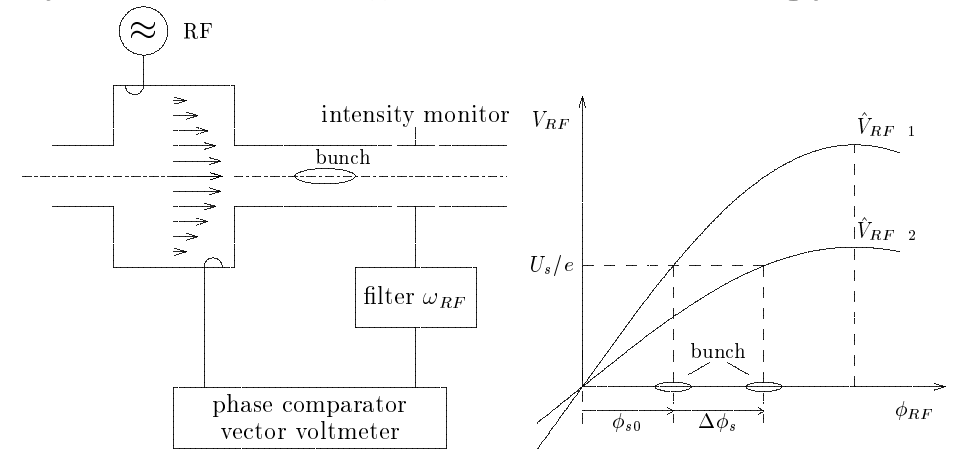
Time/frequency signal of 4 bunches

Timing signals of colliding bunches



For colliding beams it is important that the bunches meet in the interaction point where the experiment is located and where the beta functions and beam dimensions have a minimum. This is checked with intensity monitors located symmetrically on both sides of the interaction region.

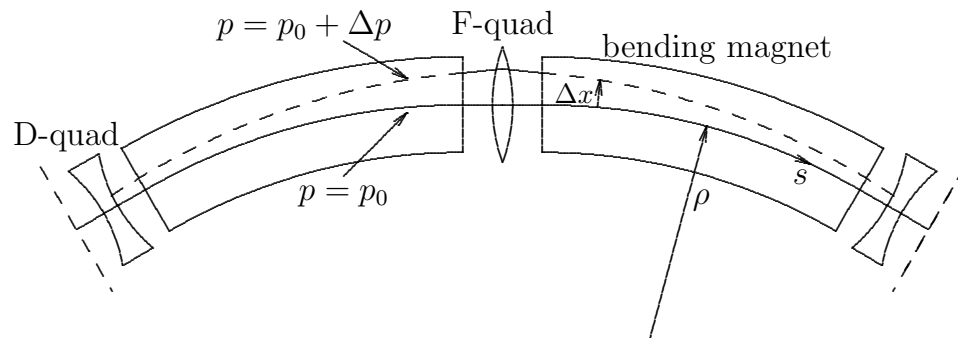
Synchronous phase and energy loss



The energy loss U_s per turn due synchrotron radiation is compensated by the RF-system with a bunch traversing cavity at synchronous phase ϕ_s satisfying $eV_{RF} \sin \phi_s = U_s$. Cable delays make absolute phase measurement difficult but we get its change versus V_{RF} by comparing cavity voltage with the one induced by bunch at ω_{RF} in intensity monitor using vector voltmeter.

$U_s \propto \int B^2 ds$ but deflection angle $\propto \int B ds$, fringe fields affect the two differently.

Energy change



A beam momentum change is made by varying RF-frequency with constant magnets

$$\frac{\Delta\omega_{RF}}{\omega_{RF}} = \frac{\Delta\omega_0}{\omega_0} = -\eta_c \frac{\Delta p}{p_0}, \quad \Delta x = D_x \frac{\Delta p}{p_0}$$

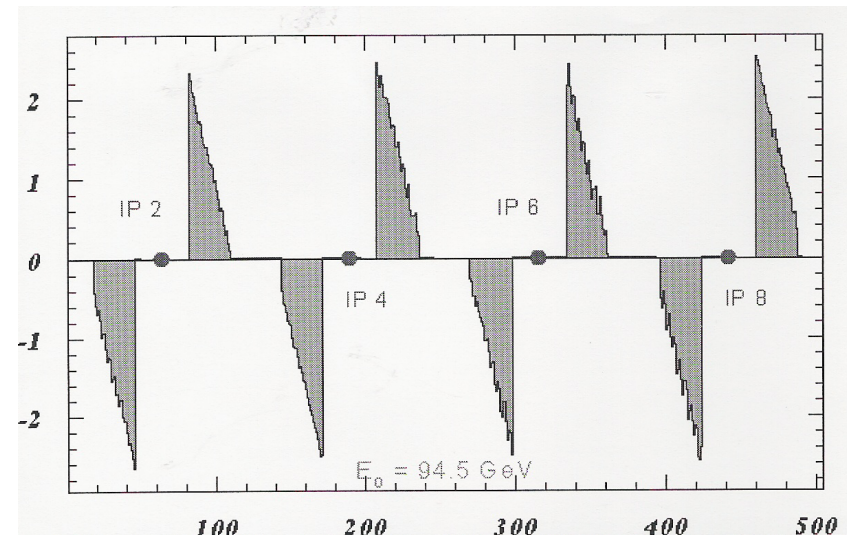
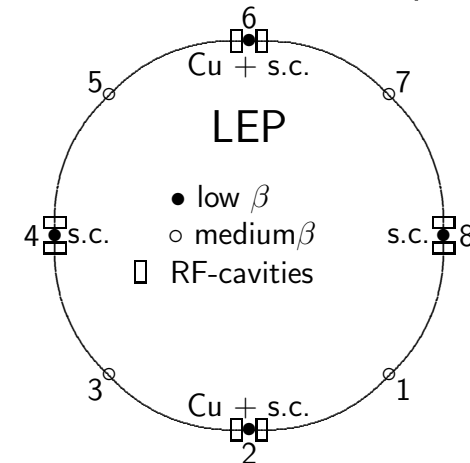
Since $C = h\lambda_{RF}$ a lower frequency forces beam on a longer orbit where energy is lower. This is used to measure energy dependent beam parameters, dispersion or chromaticity.

Dispersion measurement

Measure orbit difference for energy change, get dispersion from $\Delta x = D_x \Delta p / p_0$. Main interest D_x but there might be residual D_y .

Energy loss distribution due to S.R.

Collider e^- and e^+ lose energy in dipoles, replaced by RF. At $D_x > 0$, opposite orbit shift, shown as difference. (Anke Müller).

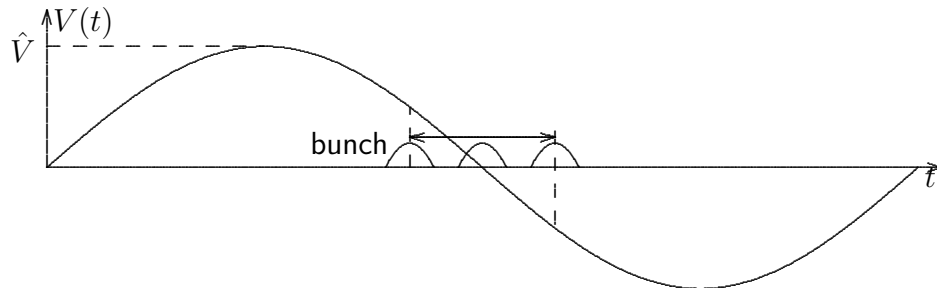


Synchrotron oscillation frequencies

Single particle incoherent oscillation with frequency ω_s , not seen by intensity monitor.

$$\omega_s = \omega_0 \sqrt{\frac{-e\eta_c h V_{RF} \cos \phi_s}{2\pi\beta^2 E_0}}, \quad \eta_c = \alpha_c - \frac{1}{\gamma^2}.$$

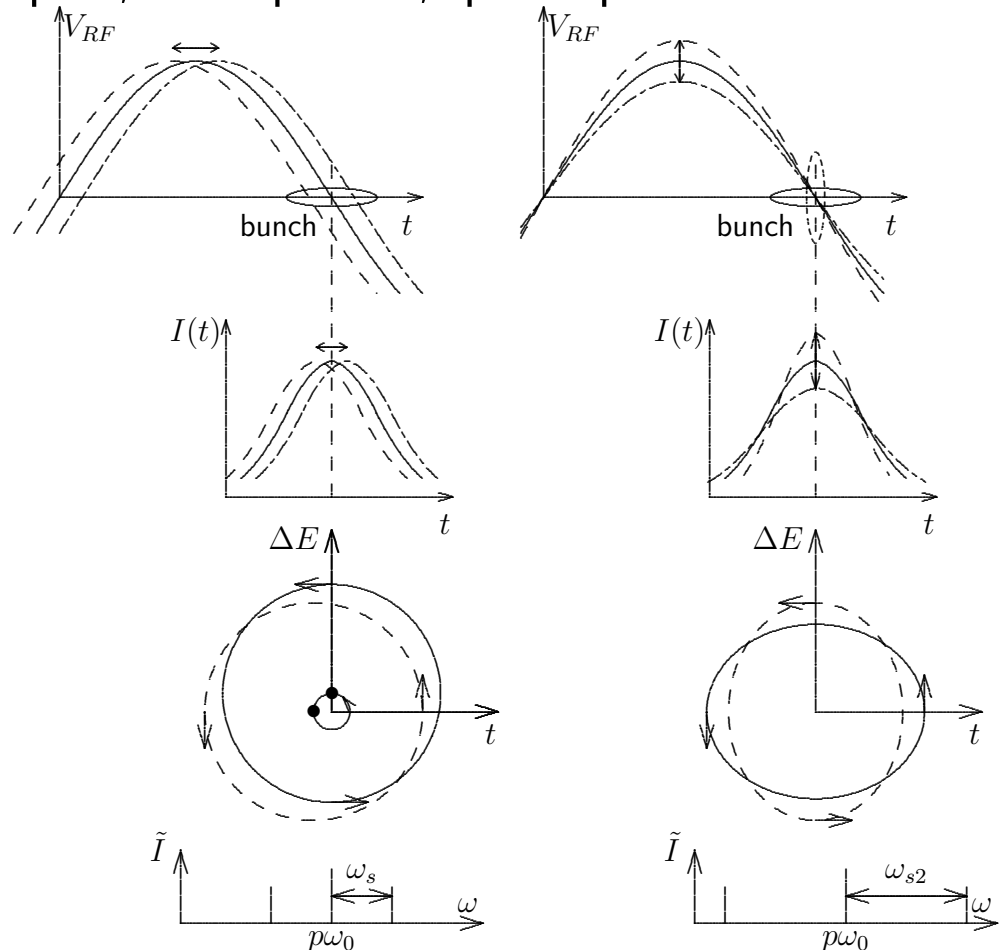
Monitor sees coherent motion, like the center-of-mass dipole mode with frequency ω_{s1}



or quadrupole oscillation between, 'short time, large energy spread', vice versa, with ω_{s2} . They represent a phase/amplitude modulation with sidebands around $p\omega_0$. Without other forces $\omega_{s1} = \omega_s$, $\omega_{s2} = 2\omega_s$ and check RF-voltage. Collective effects change these frequencies.

Injection phase error excites dipole, mismatch (wrong bunch length/energy-spread ratio) quadrupole mode; check injection.

RF-voltage modulation in phase excites dipole, in amplitude, quadrupole mode.

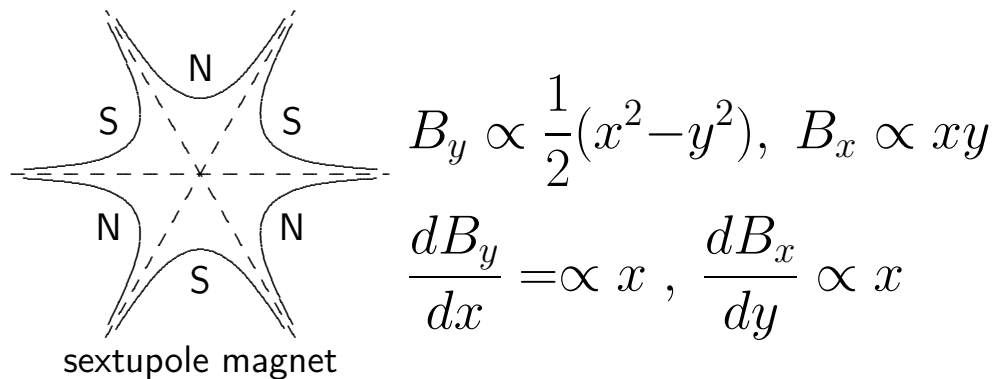


Off-energy focusing — chromaticity

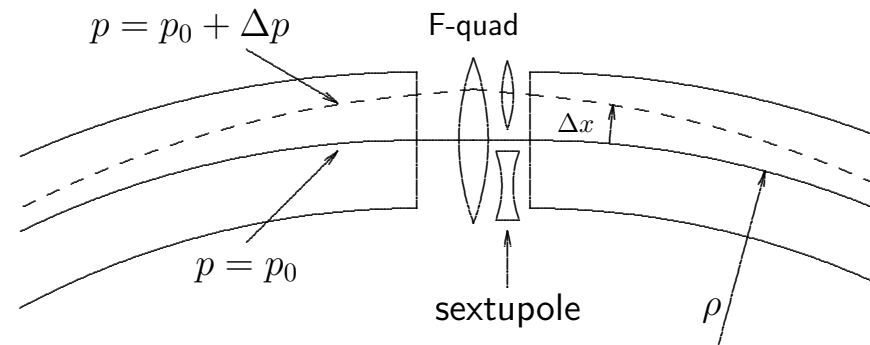
Curvature in a magnet is inversely proportional to momentum $1/\rho \propto 1/p$ giving for a higher momentum particle less focusing in quadrupoles and a tune dependence on momentum, called chromaticity which is always negative without correction.

$$Q' = \frac{\Delta Q}{\Delta p/p_0}, \quad \xi = \frac{\Delta Q/Q}{\Delta p/p_0}$$

Corrected with sextupoles at finite dispersion.



The local sextupole field is in the horizontal plane a quadrupole of strength $\propto x$, in the vertical plane it is a rotated quadrupole.



Sextupoles are installed at places of finite dispersion. A particle with excess energy is focused less by the quad but, since it is displaced to the outside, gets extra focusing by the sextupole as compensation.

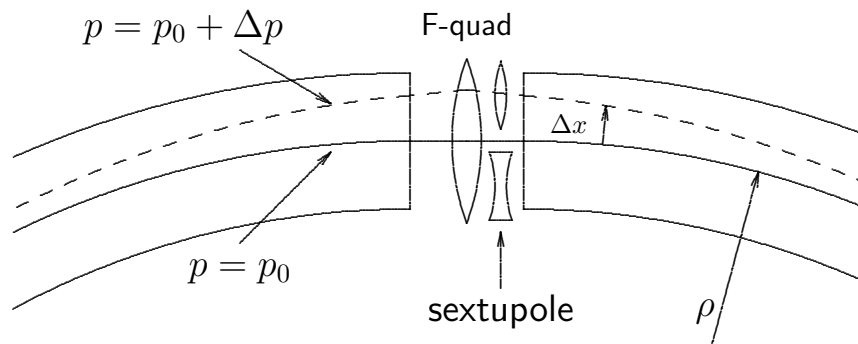
Without chromatic correction the energy oscillation of a particle makes a tune modulation and can cross resonances. Furthermore an instability, called 'head-tail' can occur.

Sextupoles are non-linear elements which can create resonances and limit dynamic aperture and have to be distributed such as to limit these effects.

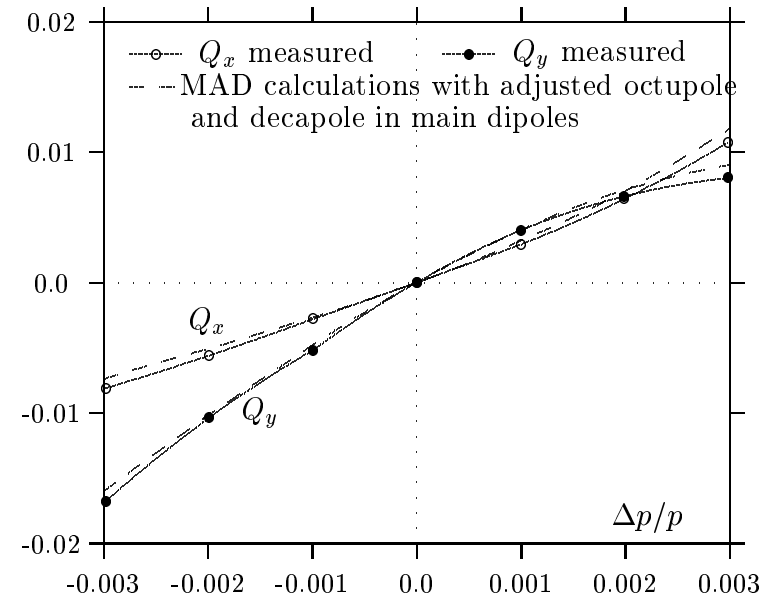
Measure chromaticity

Chromaticity and change of momentum

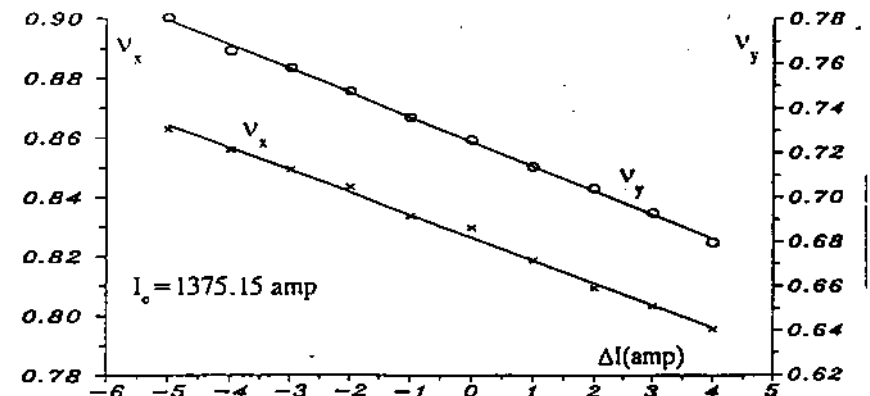
$$Q' = \frac{dQ}{dp/p}, \quad \frac{dp}{p} = -\frac{1}{\eta_c} \frac{d\omega_{RF}}{\omega_{RF}}$$



To get the chromaticity we measure the tunes as a function of f_{RF} . This is done with the sextupoles on for the corrected and with them turned off for the natural chromaticity. The latter is also obtained by varying momentum through a dipole field change but keeping the beam on the nominal orbit going through the sextupole centers where they have no influence, this is based on $dp/p_0 = dB/B_0$.

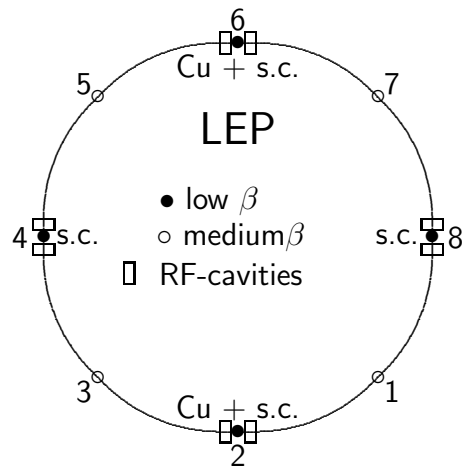


Measured and calculated Q vs. Δp , LEP

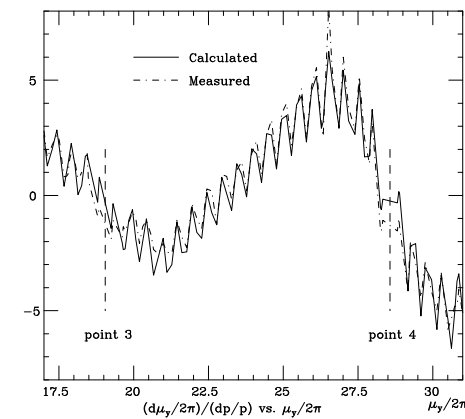
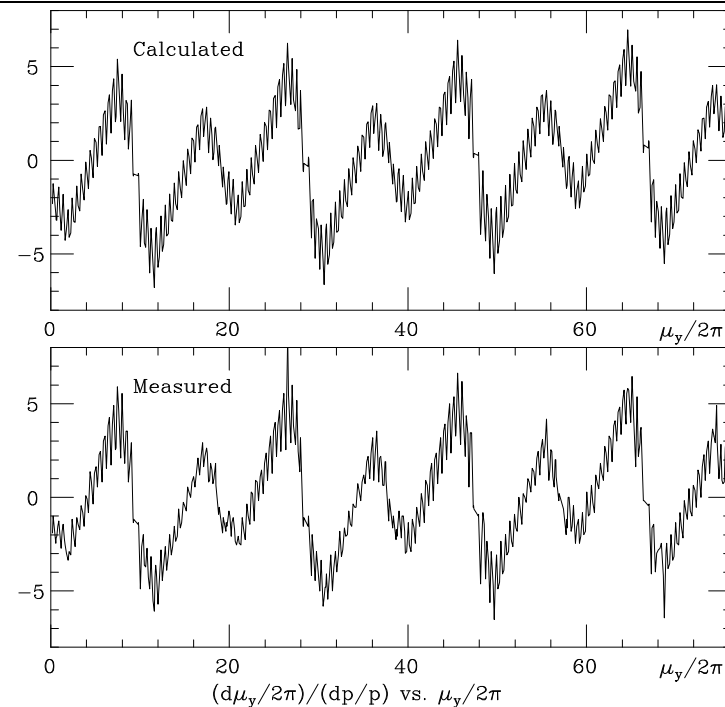


Natural Q' measured by changing dipole field in SPEAR (H. Wiedemann).

Chromatic phase advance $d\mu/(dp/p)$



Large rings, specially colliders, have long dispersion-free straight section with strong focusing. The chromaticity created there is only corrected where $D_x > 0$ and builds-up before reaching this. Measuring betatron phase advance for different energy deviations gives chromatic phase advance and checks the chromatic correction. LEP example show saw-tooth of local chromaticity but vanishing over the whole ring. Mismatched off-energy orbit shows fine structure by beta beating.



3) COLLECTIVE EFFECTS

Longitudinal Overview

The single particle motion is given by external guide fields, dipoles, quadrupoles, RF, etc.

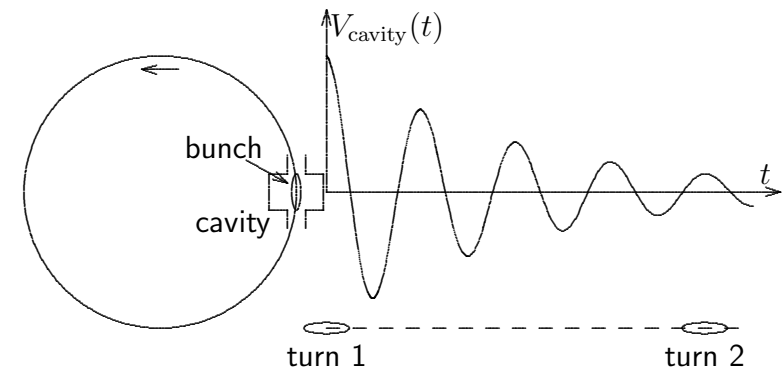
Beam with many particles induces currents in vacuum chamber **impedance** and creates **self fields** acting back on it. This **collective** action can: give **synchrotron frequency shift** by modified focusing, increase initial disturbance, **instability**, **change particle distribution**.

Multi-turn effects driven by narrow-band cavity with memory build up instability in many turns with small self-fields treated as **perturbation**

Start a small disturbance from a stationary beam, calculate fields this produces through impedance and check if they increase/decrease the initial amplitude, gives growth/damping rate. Check this for orthogonal (independent) modes of disturbances.

cas08dia-32

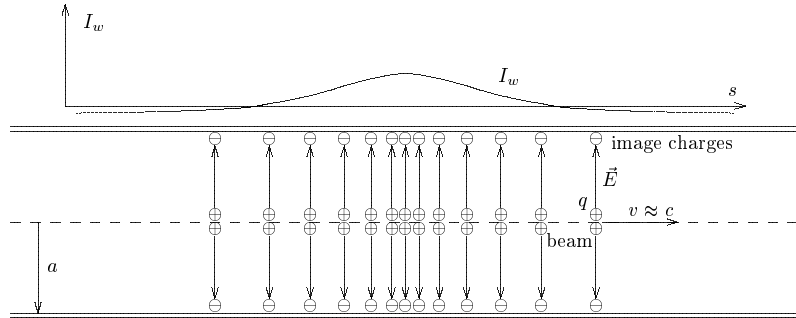
Bunch induces fields in passive cavity which oscillate and act back next turn, in/decreasing original disturbance depending on phase.



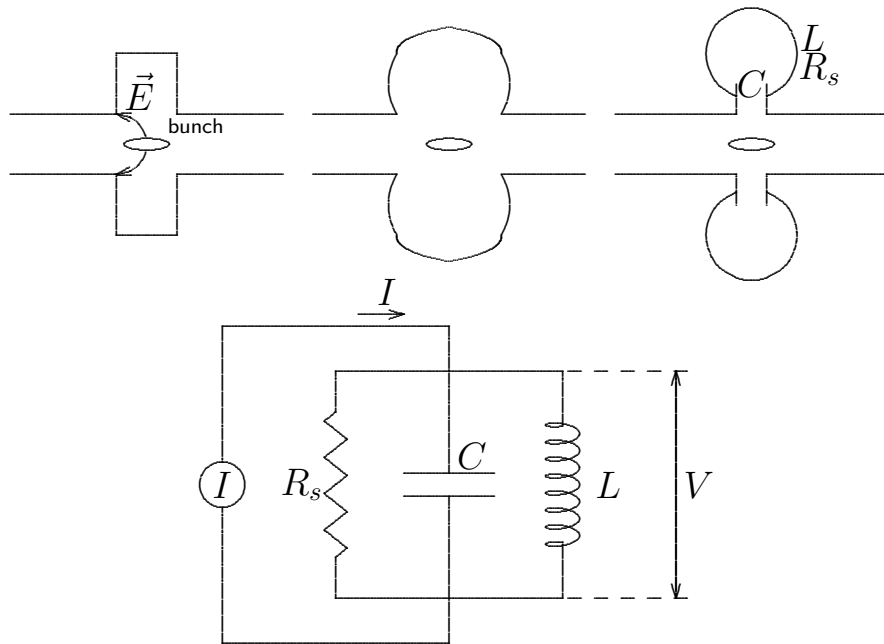
Single traversal effects driven by strong self-fields from broad impedances change distribution, modify oscillation modes and can couple them. Self consistent solutions are difficult to get, **bunch lengthening**.

Wake function and impedance

Resonator



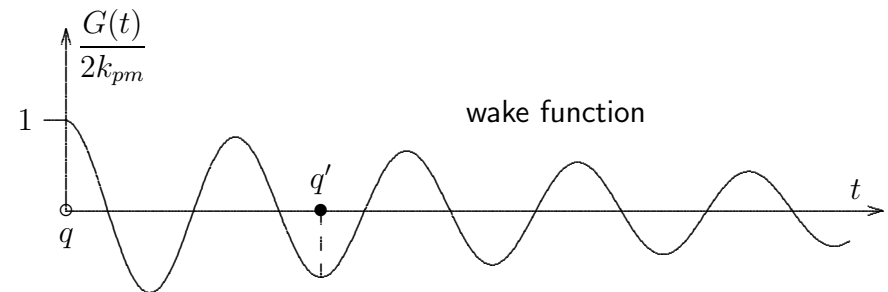
Beam induces wall current $I_w = -(I_b - \langle I_b \rangle)$



Cavities have narrow oscillation modes which drive coupled bunch instabilities. Each resembles an **RCL - circuit** and is treated as such. This circuit has shunt impedance R_s , inductance L , capacity C . Since they cannot be identified related parameters are used and measured directly: **resonance frequency** ω_r , **quality factor** Q , **damping rate** α_s :

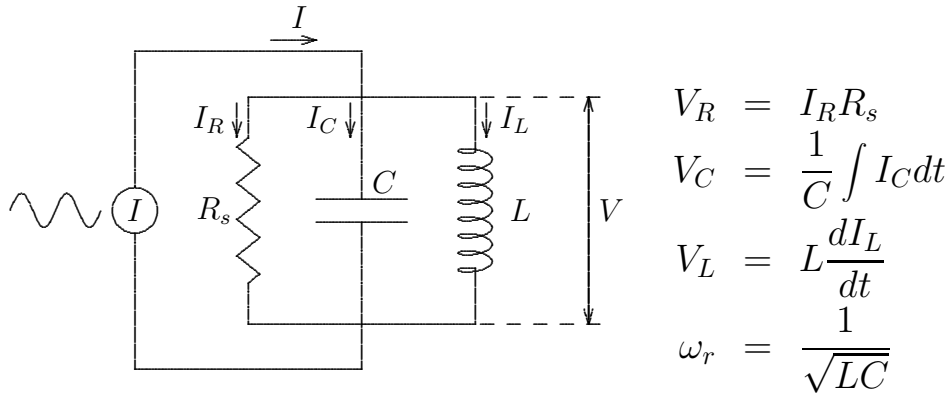
$$\omega_r = \frac{1}{\sqrt{LC}}, \quad Q = R_s \sqrt{\frac{C}{L}} = \frac{R_s}{L\omega_r} = R_s C \omega_r$$

$$\alpha_s = \frac{\omega_r}{2Q}, \quad L = \frac{R_s}{Q\omega_r}, \quad C = \frac{Q}{\omega_r R_s}.$$



Impedance

Driving circuit with current $I = \hat{I} \cos(\omega t)$



$$V_R = V_C = V_L = V, \quad I_R + I_C + I_L = I$$

$$\dot{I} = \dot{I}_R + \dot{I}_C + \dot{I}_L = \frac{\dot{V}}{R_s} + C\ddot{V} + \frac{V}{L}$$

using $L = R_s/(\omega_r Q)$ and $C = Q/(\omega_r R_s)$

$$\ddot{V} + \frac{\omega_r}{Q} \dot{V} + \omega_r^2 V = \frac{\omega_r R_s}{Q} \dot{I}$$

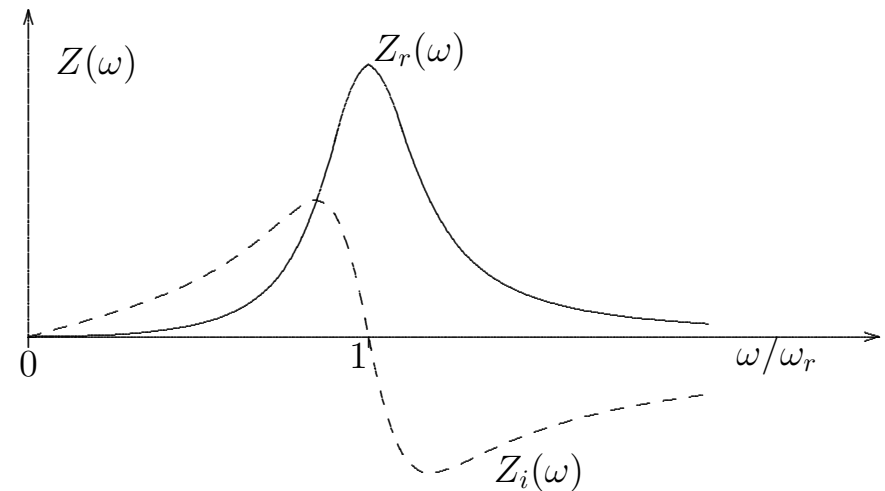
Seeking harmonic solution

$$V(t) = \hat{I} R_s \frac{\cos(\omega t) + Q \frac{\omega^2 - \omega_r^2}{\omega_r \omega} \sin(\omega t)}{1 + Q^2 \left(\frac{\omega^2 - \omega_r^2}{\omega_r \omega} \right)^2}$$

Has cosine term **in phase** with exciting current, absorbs energy, **resistive**. Sine term is **out of phase**, does not absorb energy, **reactive**. Ratio between voltage and current is **impedance as function of frequency** ω

$$Z_r = \frac{R_s}{1 + Q^2 \left(\frac{\omega_r^2 - \omega^2}{\omega_r \omega} \right)^2}, \quad Z_i = \frac{-R_s Q \frac{\omega^2 - \omega_r^2}{\omega_r \omega}}{1 + Q^2 \left(\frac{\omega^2 - \omega_r^2}{\omega_r \omega} \right)^2}.$$

in complex notation $Z(\omega) = Z_r(\omega) + j Z_i(\omega)$. Resistive part $Z_r(\omega) \geq 0$, reactive part $Z_i(\omega)$ positive below, negative above ω_r .



Induced voltage and energy loss by a stationary bunch

Circulating symmetric bunch (N_b particles) has current

$$I(t) = I_0 + 2 \sum I_p \cos(p\omega_0 t), \quad I_p = \int_0^{T_0} I(t) \cos(p\omega_0 t) dt$$

In impedance $Z(\omega)$ it induces voltage

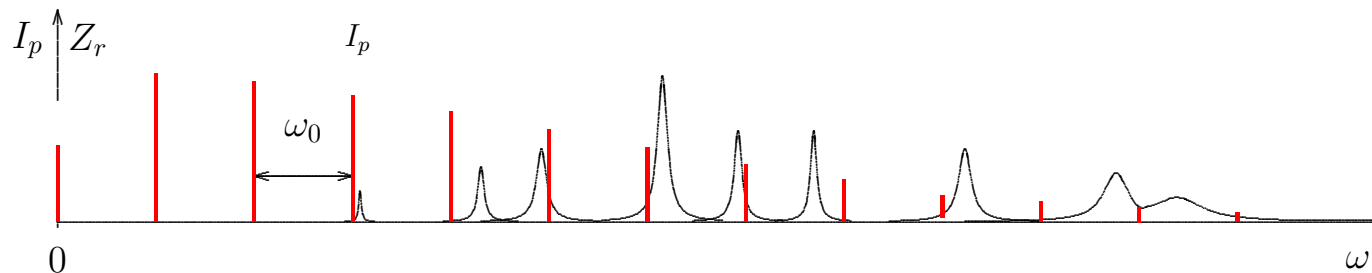
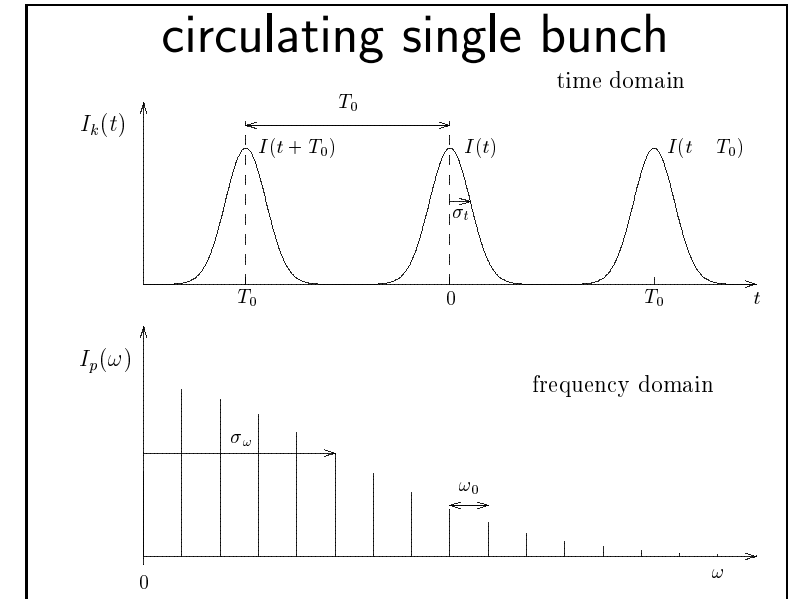
$$V(t) = \sum I_p [Z_r(p\omega_0) \cos(p\omega_0 t) - Z_i(p\omega_0) \sin(p\omega_0 t)]$$

Energy lost per particles and turn $U = \int_0^{T_0} I(t)V(t)dt/N_b$

$$U = \frac{2T_0}{N_b} \sum_1^\infty I_p^2 Z_r(p\omega_0) = \frac{2e}{I_0} \sum_1^\infty I_p^2 Z_r(p\omega_0)$$

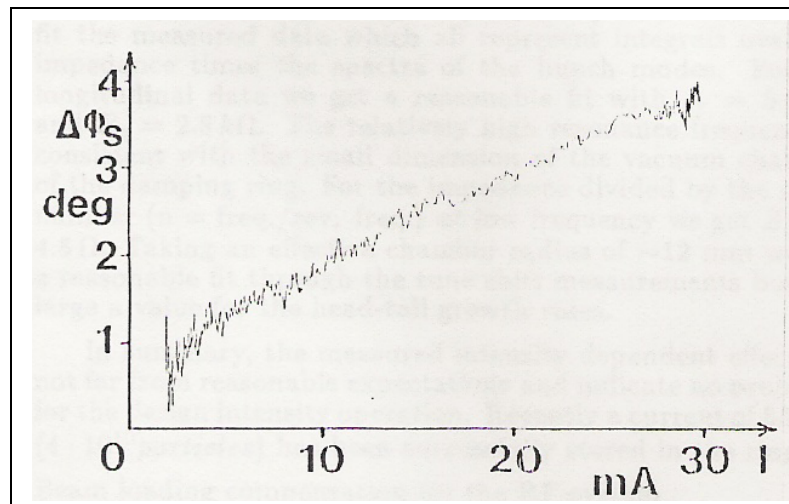
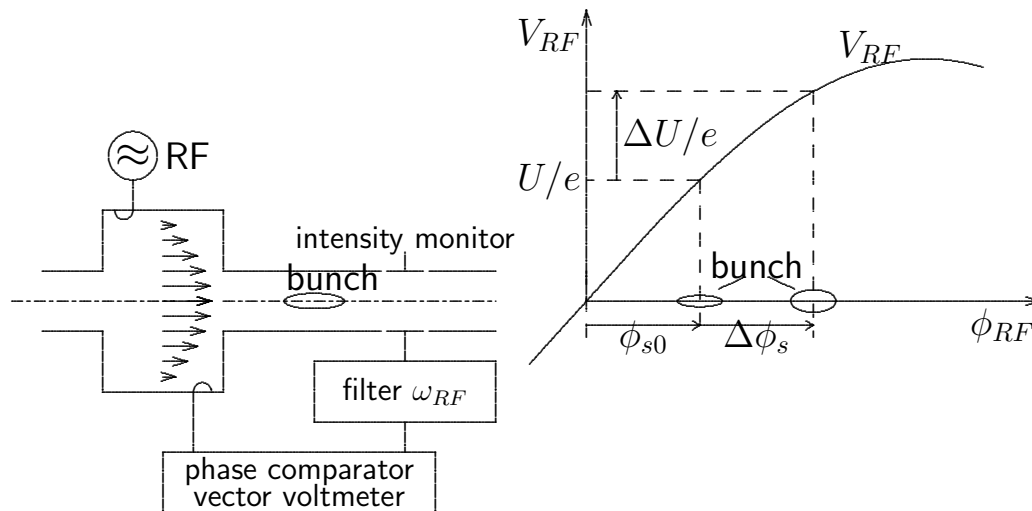
using $\int_0^{T_0} \cos(p'\omega_0 t) \sin(p\omega_0 t) dt = 0, \quad I_0 = eN_b/T_0$

$$\int_0^{T_0} \cos(p'\omega_0 t) \cos(p\omega_0 t) dt = \begin{cases} T_0/2 & \text{for } p' = p \\ 0 & \text{for } p' \neq p \end{cases}$$



Measuring energy loss

$$U = \frac{2T_0}{N_b} \sum_1^\infty I_p^2 Z_r(p\omega_0) \approx \frac{2}{N_b} \int_0^\infty |\tilde{I}^2(\omega)| Z_r(\omega) d\omega$$

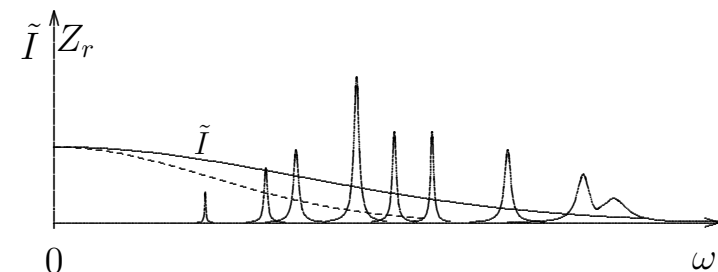


SLAC
damping
ring

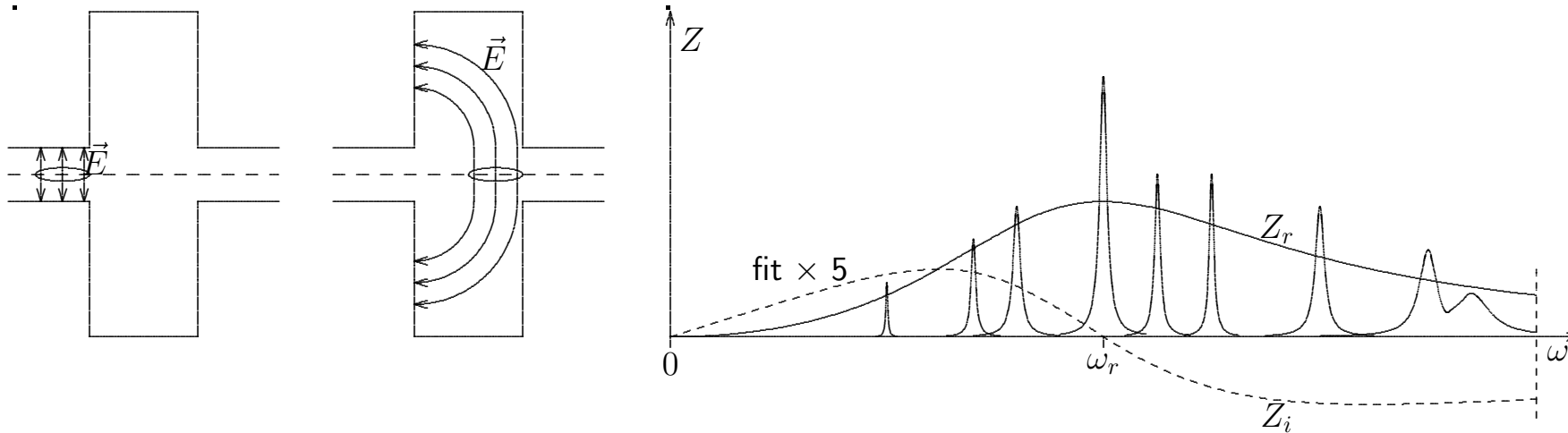
Comparing the phase of the bunch signal with the one of the RF is difficult if there are many cavities. Also, at higher currents signals are larger, warm up the cable and expand it, leading to a current dependent delay.

A method developed at DESY avoids this by comparing the distance between two adjacent bunches as a function of the current in the second.

Measuring the energy loss for different bunch length helps to get information of the frequency dependence of the impedance.



Typical ring impedance



Aperture changes form cavity-like objects with ω_r , R_s and Q and impedance $Z(\omega)$ developed for $\omega < \omega_r$, where it is inductive

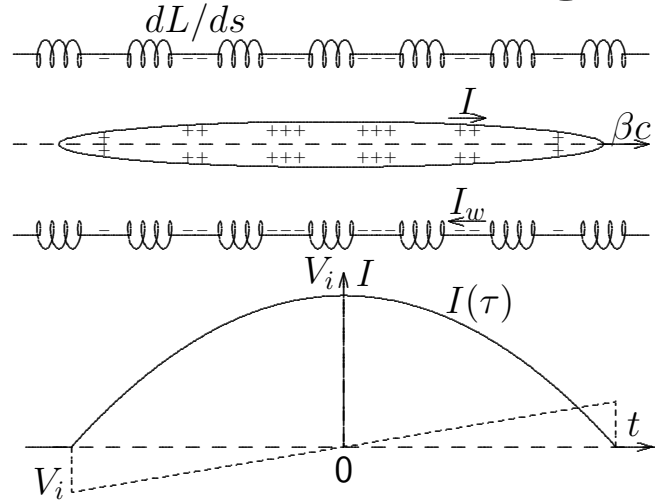
$$Z(\omega) = R_s \frac{1 - jQ \frac{\omega^2 - \omega_r^2}{\omega \omega_r}}{1 + \left(Q \frac{\omega^2 - \omega_r^2}{\omega \omega_r} \right)^2} \approx j \frac{R_s \omega}{Q \omega_r} + \dots$$

Sum impedance at $\omega \ll \omega_{rk}$ divided by mode number $n = \omega/\omega_0$ is with inductance L

$$\left| \frac{Z}{n} \right|_0 = \sum_k \frac{R_{sk} \omega_0}{Q_k \omega_{rk}} = L \omega_0 = L \frac{\beta c}{R}.$$

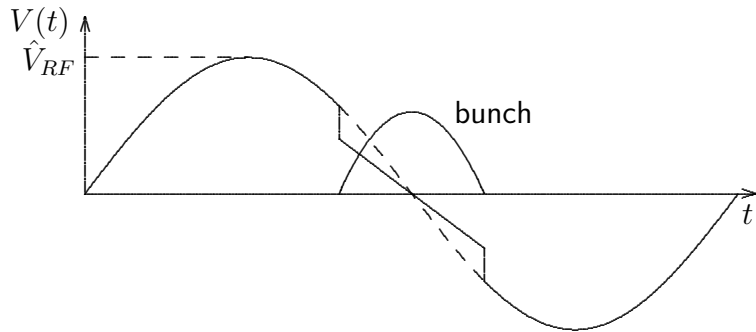
It depends on impedance per length, $\approx 15 \Omega$ in older, 1Ω in newer rings. The shunt impedances R_{sk} increase with ω up to cut-off frequency where wave propagation starts and become wider and smaller. A broad band resonator fit helps to characterize impedance giving Z_r , Z_i , $G(t)$ useful for single traversal effects. However, for multi-traversal instabilities narrow resonances at ω_{rk} must be used.

Potential well bunch lengthening



$$E_z = -\frac{dL}{dz} \frac{dI_w}{dt} = \frac{dL}{dz} \frac{dI_b}{dt}$$

$$V = -\int E_z dz = -L \frac{dI_b}{d\tau}$$



We take a parabolic bunch form

$$I_b(\tau) = \hat{I} \left(1 - \frac{\tau^2}{\hat{\tau}^2}\right) = \frac{3\pi I_0}{2\omega_0 \hat{\tau}} \left(1 - \frac{\tau^2}{\hat{\tau}^2}\right)$$

$$\frac{dI_b}{d\tau} = -\frac{3\pi I_0 \tau}{\omega_0 \hat{\tau}^3}, \quad I_0 = \langle I_b \rangle,$$

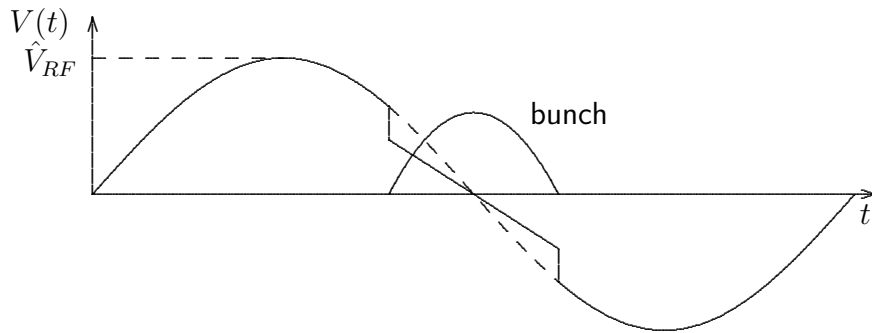
$$V = \hat{V} (\sin \phi_s + h\omega_0 \cos \phi_s \tau) + \frac{3\pi I_0 L \tau}{\omega_0 \hat{\tau}^3}$$

$$V = \hat{V} \left[\sin \phi_s + \cos \phi_s h\omega_0 \left(1 + \frac{3\pi |Z/n|_0 I_0}{h\hat{V} \cos \phi_s (\omega_0 \hat{\tau})^3}\right) \tau \right]$$

$$\omega_{s0}^2 = -\frac{\omega_0^2 h \eta_c e \hat{V} \cos \phi_s}{2\pi E}$$

$$\omega_s^2 = \omega_{s0}^2 \left[1 + \frac{3\pi |Z/n|_0 I_0}{h\hat{V}_{RF} \cos \phi_s (\omega_0 \hat{\tau})^3} \right]$$

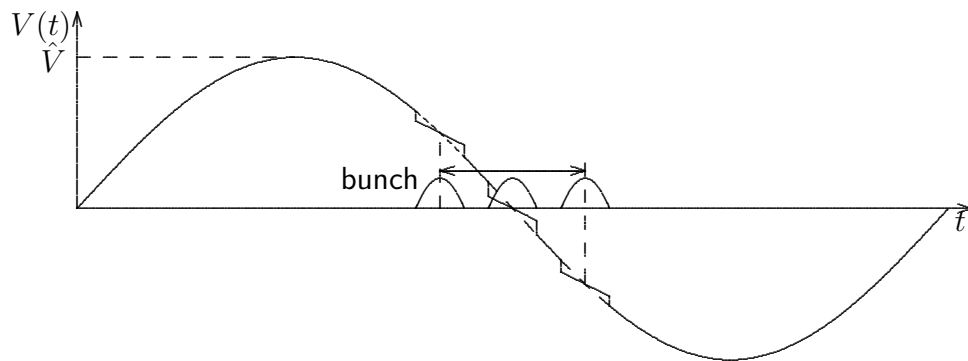
$$\frac{\Delta\omega_s}{\omega_0} = \frac{\omega_s - \omega_{s0}}{\omega_{s0}} \approx \frac{3\pi |Z/n|_0 I_0}{2h\hat{V}_{RF} \cos \phi_s (\omega_0 \hat{\tau}_0)^3}$$



$$\frac{\omega_s^2}{\omega_{s0}^2} = 1 + \frac{3\pi|Z/n|_0 I_0}{h\hat{V}_{RF} \cos \phi_s (\omega_0 \hat{\tau})^3}$$

$$\frac{\omega_s - \omega_{s0}}{\omega_{s0}} = \frac{\Delta\omega_s}{\omega_s} \approx \frac{3\pi|Z/n|_0 I_0}{2h\hat{V} \cos \phi_s (\omega_0 \hat{\tau}_0)^3}$$

Only incoherent frequency ω_s of single particles is changed (reduced $\gamma > \gamma_T$, increased $\gamma < \gamma_T$), not coherent dipole (rigid bunch) frequency ω_{s1} . The two get separated.



Decreasing ω_s reduces longitudinal focusing, increases bunch length $\hat{\tau}$. Relative energy spread $\hat{\epsilon} = \hat{\tau}\omega_s/\eta_c$ is given for electrons by synchrotron radiation, for protons the product (emittance) $\hat{\tau}\hat{\epsilon} = \text{const.}$

$$\text{electron } \frac{\Delta\hat{\tau}}{\hat{\tau}_0} = -\frac{\Delta\omega_s}{\omega_{s0}}, \text{ proton } \frac{\Delta\hat{\tau}}{\hat{\tau}_0} = -\frac{\Delta\omega_s}{2\omega_{s0}}$$

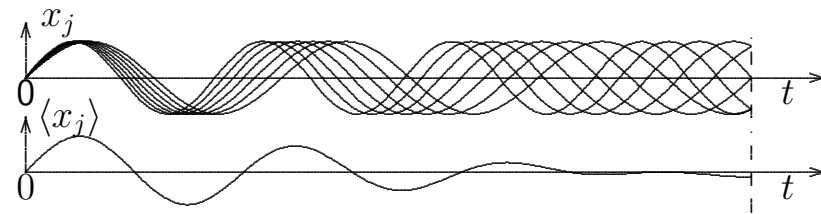
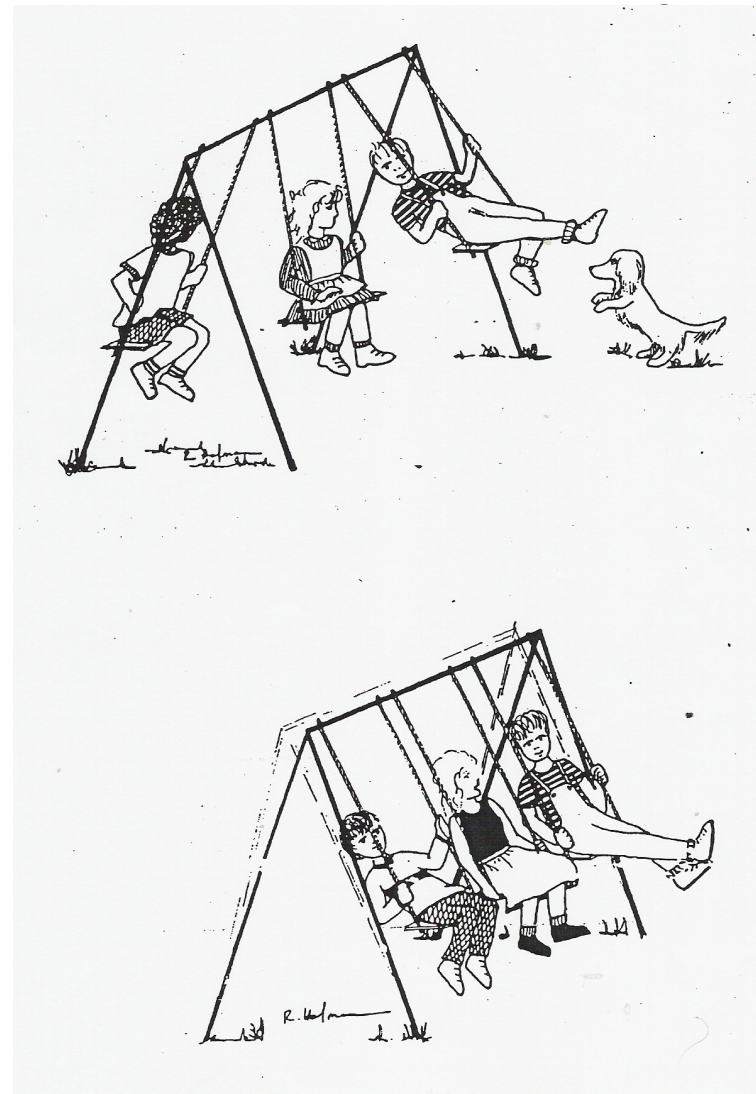
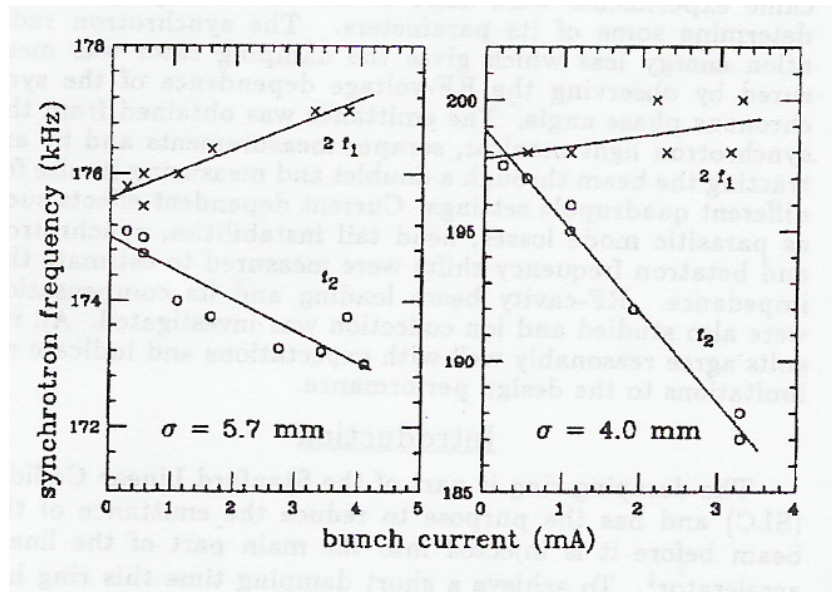
From observed bunch lengthening impedance is estimated.

Frequency measurement would be better, but ω_s is invisible and ω_{s1} does not move, however, quadrupole mode can be used

$$\frac{\omega_{s2} - 2\omega_{s0}}{2\omega_{s0}} = \frac{\Delta\omega_{s2}}{\omega_{s2}} \approx \frac{1}{4} \frac{\Delta\omega_s}{\omega_{s0}}.$$

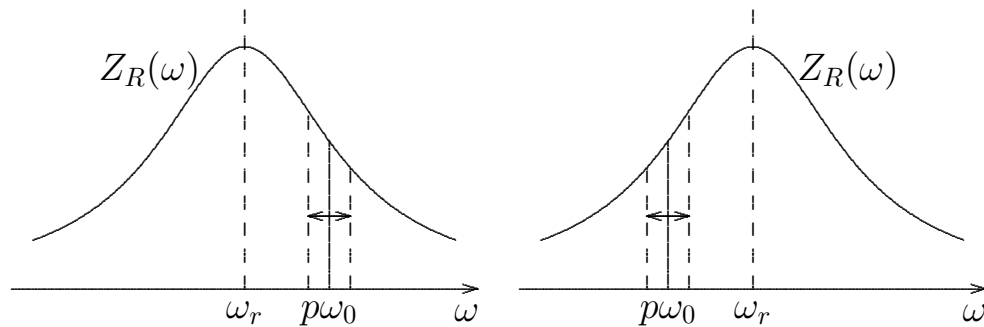
Measurements of ω_{s1} and ω_{s2}

The measurement of the dipole and quadrupole synchrotron frequencies as a function of current gives an easy estimate of the reactive longitudinal impedance. Since the RF-voltage might change a little with current due to beam loading the observation of ω_1 might serve as calibration. This is evident from the measurement at the SLAC damping ring for two different bunch lengths.



Robinson instability

Qualitative treatment

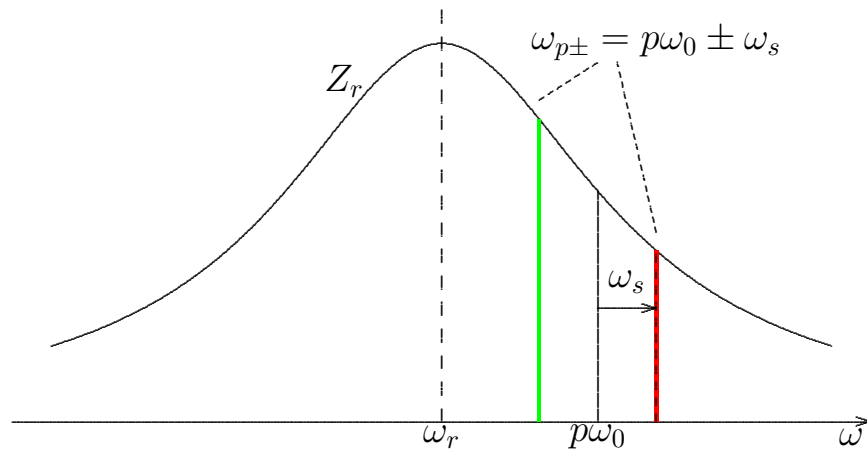


Important longitudinal instability of a bunch interacting with a narrow impedance, called **Robinson** instability. In a qualitative approach we take single bunch and a narrow-band cavity of resonance frequency ω_r and impedance $Z(\omega)$ taking only its resistive part Z_r . The revolution frequency ω_0 depends on energy deviation ΔE

$$\frac{\Delta\omega_0}{\omega_0} = -\eta_c \frac{\Delta p}{p}.$$

While the bunch is executing a coherent dipole mode oscillation $\epsilon(t) = \hat{\epsilon} \cos(\omega_s t)$ its energy and revolution frequency are modulated. **Above transition** ω_0 is **small** when the **energy is high** and ω_0 is **large** when the **energy is small**. If the cavity is tuned to a resonant frequency slightly smaller than the RF-frequency $\omega_r < p\omega_0$ the bunch sees a higher impedance and **loses more energy** when it has an **energy excess** and it **loses less energy** when it has a **lack of energy**. This leads to a **damping** of the oscillation. If $\omega_r > p\omega_0$ this is reversed and leads to an **instability**. Below transition energy the dependence of the revolution frequency is reversed which changes the stability criterion.

Frequency domain, only one harmonic p



$$\epsilon = \hat{\epsilon} e^{-\alpha_s t} \sin(\omega_s t), \text{ damping if } \alpha_s > 0$$

$$\alpha_s = \frac{\omega_{s0} p I_p^2 (Z_r(\omega_{p+}) - Z_r(\omega_{p-}))}{2 I_0 h \hat{V} \cos \phi_s}$$

$\gamma > \gamma_T$, $\cos \phi_s < 0$, stable $Z_r(\omega_{p-}) > Z_r(\omega_{p+})$

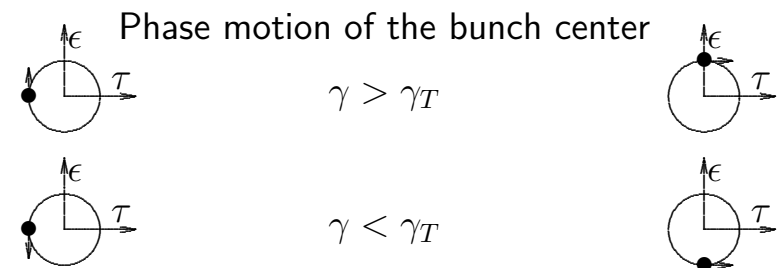
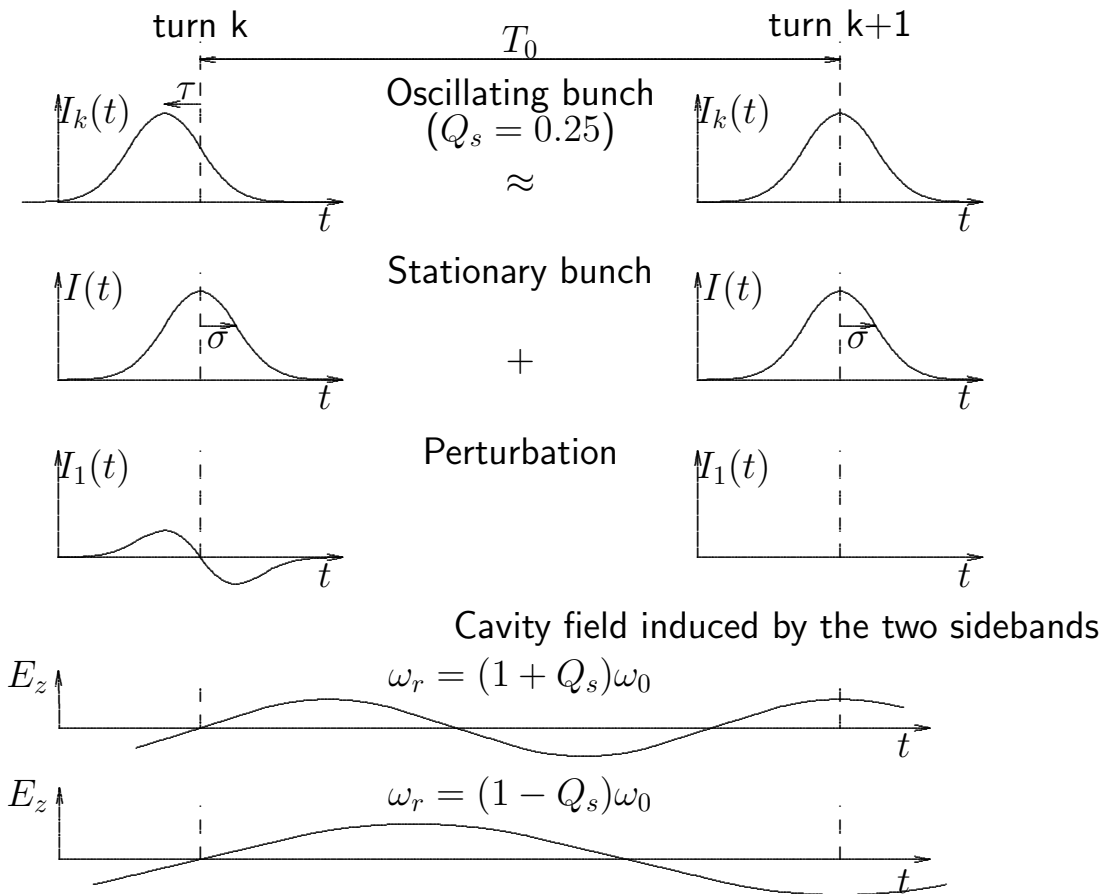
Damping rate $\propto Z_r$ difference at side-bands.

RF-cavity: $p = h$, $I_p \approx I_0$.

$$\alpha_s \approx \frac{\omega_{s0} I_0 (Z_r(\omega_{p+}) - Z_r(\omega_{p-}))}{2 \hat{V} \cos \phi_s}$$

$$\text{general } \alpha_s = \sum_p \frac{\omega_{s0} p I_p^2 (Z_r(\omega_{p+}) - Z_r(\omega_{p-}))}{2 I_0 h \hat{V} \cos \phi_s}$$

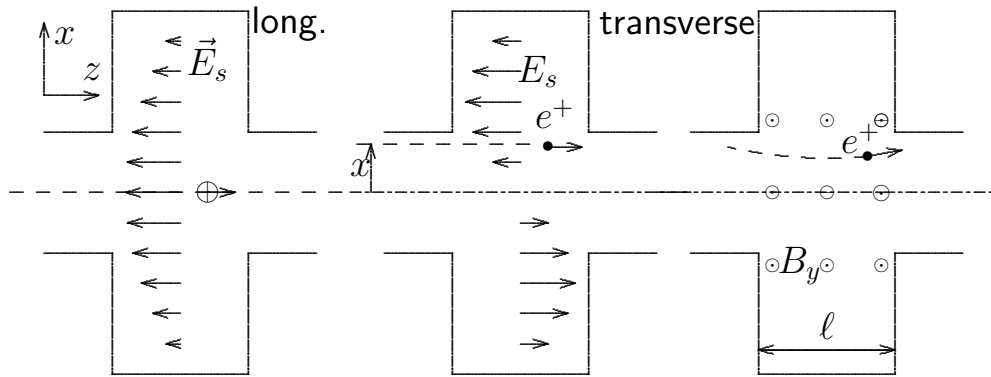
Qualitative understanding



Narrow band \rightarrow long memory, vice-versa

Transverse collective effects

Transverse impedance



Field excited by $Ix = D = \hat{D} \cos(\omega t)$

$$\frac{\partial E_z}{\partial x} = -kIx, \quad E_z(x) = -kIx^2$$

$$Z_L(x) = -\int E_z dz / I = -E_z \ell / I = k\ell x^2$$

$$\oint \vec{B} d\vec{a} = -\oint \vec{E} d\vec{s}, \quad \dot{B}_y x \ell = E_z \ell = -k\ell D x$$

$$\dot{B}_y = -k\hat{D} \cos(\omega t), \quad B = -k\hat{D} \sin(\omega t) / \omega$$

field B out of phase with $D = Ix$

$$\hat{B}_y = -k\hat{D} / \omega, \quad \text{Lorentz force } \hat{F} \approx -ec\hat{B}_y$$

$$Z_T = -\frac{F_x \ell}{e\hat{D}} = \frac{ck\ell}{\omega} = \frac{cZ_L}{x^2\omega} = \frac{c}{2\omega} \frac{d^2 Z_L}{dx^2}.$$

Used special case to define transverse impedance and its relation to second derivative of the longitudinal impedance of same mode. In General we have the impedances long.: integrated field/current; trans.: integrated defl. field/ dipole moment On resonance, E_z is in, B_y out of phase of I . General deflecting mode, using $x = \hat{x}e^{j\omega t}$

$$Z_T(\omega) = j \frac{\int (\vec{E}(\omega) + [\vec{v} \times \vec{B}(\omega)])_T ds}{Ix(\omega)}$$

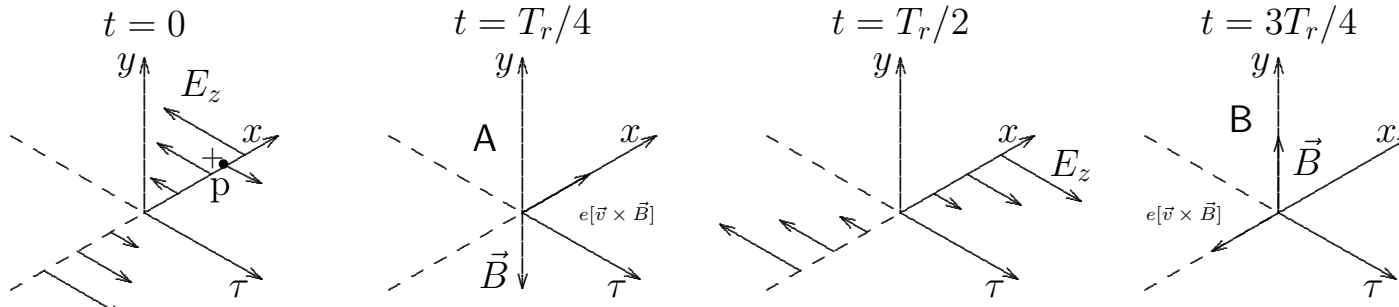
Relation Z_L to Z_T of different modes:

In ring of global and vacuum chamber radii R and b the impedances, averaged for different modes, have semi-empirical ratio

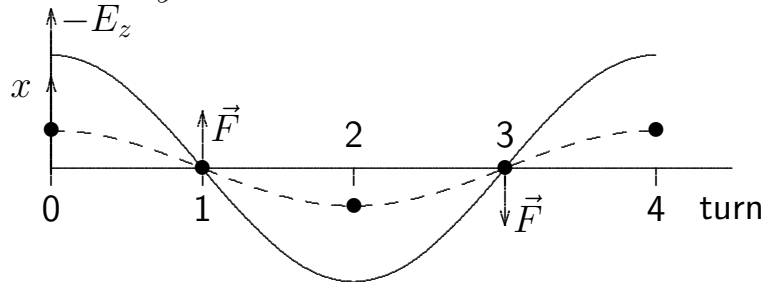
$$Z_T(\omega) \approx \frac{2R}{b^2} \frac{Z_L(\omega)}{\omega / \omega_0}$$

From area available for the wall current we expect $Z_L \propto 1/b$, therefore $Z_T \propto 1/b^3$.

Transverse multi-traversal instability of a single bunch

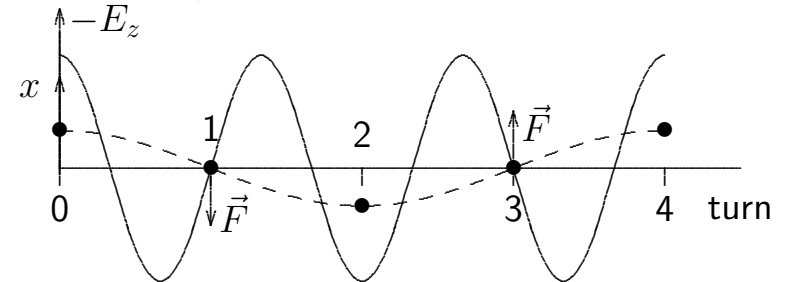


A bunch p traverses a cavity with off-set x , excites a field $-E_z$ which converts after $T_r/4$ into field $-B_y$, then into E_z and after into B_y .



A) Cavity is tuned to upper sideband. Next turn bunch traverses in situation 'A', $t = T_r/4$) with velocity in $-x$ -direction and gets by B_y force in $+x$ -direction which damps oscillation.

The bunch oscillates with tune Q having a fractional part $q = 1/4$ seen as sidebands at $\omega_0(\text{integer} \pm q)$ by a stationary observer.



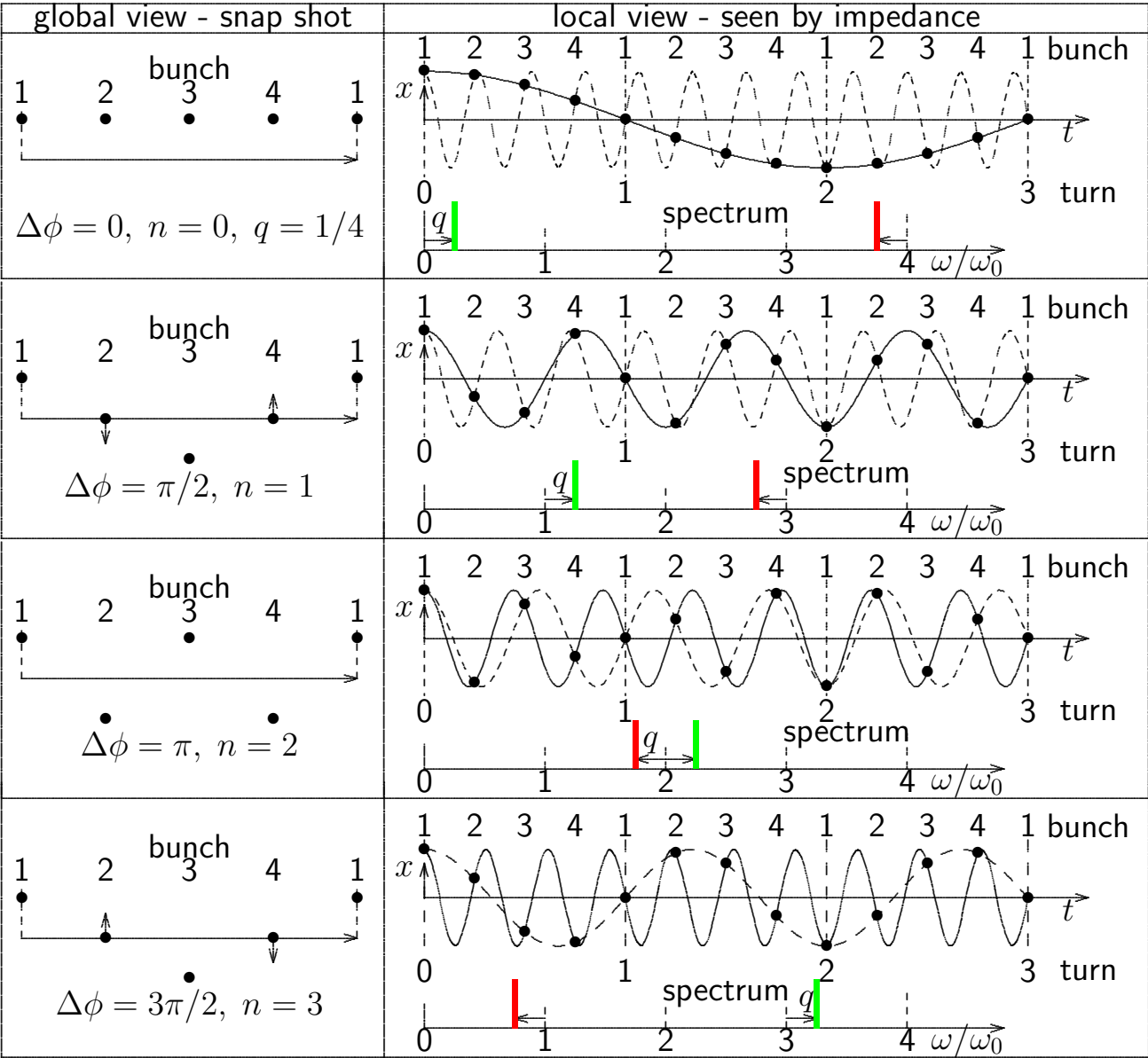
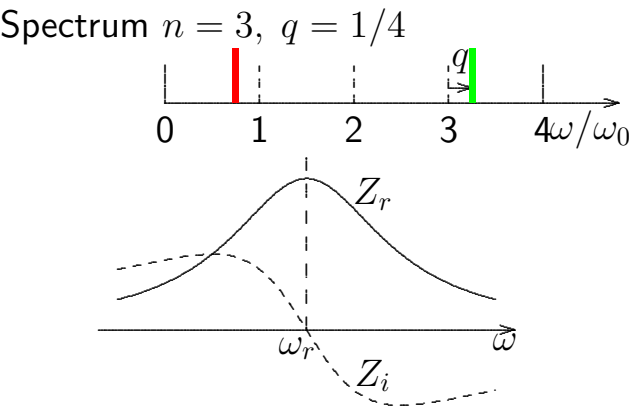
B) Cavity is tuned to lower sideband, bunch traverses next in situation 'B', $t = T_r 3/4 = T_r(1 - 1/4)$ with negative velocity and force in same direction, increases velocity, instability.

$$\text{damping rate } a = \frac{e\omega_0\beta_x}{4\pi m_0 c^2 \gamma I_0} \sum_{\omega > 0} (I_{p+}^2 Z_{Tr}(\omega_{p+}) - I_{p-}^2 Z_{Tr}(\omega_{p-})), \quad \omega_{p\pm} = \omega_0(p \pm q).$$

Transverse instability of many bunches

M bunches can oscillate in M independent modes $n = M\Delta\phi/2\pi$, phase $\Delta\phi$ between them seen in global view. Locally, bunches pass with increasing time delay shown as bullets fitted by upper (solid) and lower (dashed) side-band frequency. Higher frequencies can be fitted and spectrum repeats every $4\omega_0$.

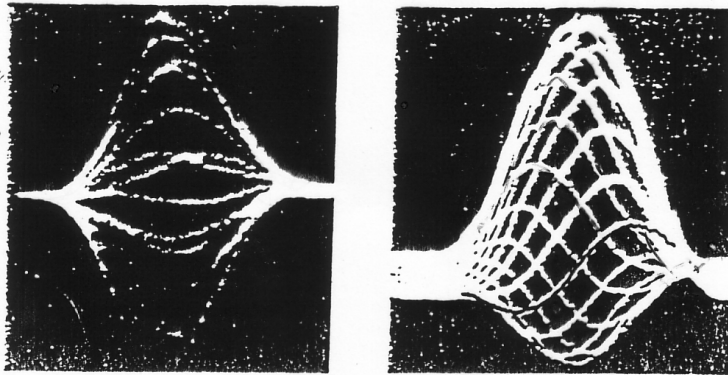
$$\omega_{p\pm} = \omega_0(pM \pm (n + q))$$



Head-tail mode oscillation

Synchrotron motion in ΔE and τ affect transverse motion via chromaticity $Q' = dQ/(dp/p)$. For $\gamma > \gamma_T$ has excess energy moving from head to tail and lack going from tail to head. For $Q' > 0$, phase advances in first and lags in second step; vice versa for $Q' < 0$ or $\gamma < \gamma_T$.

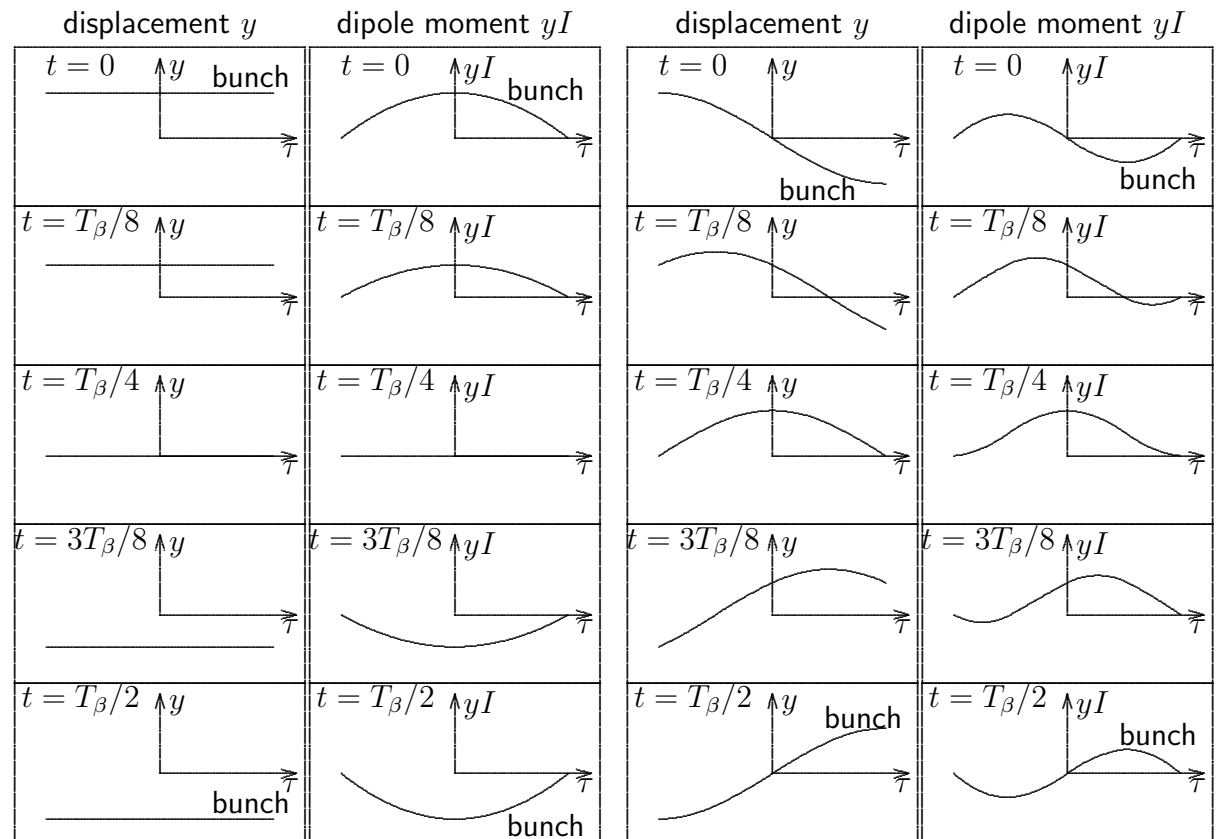
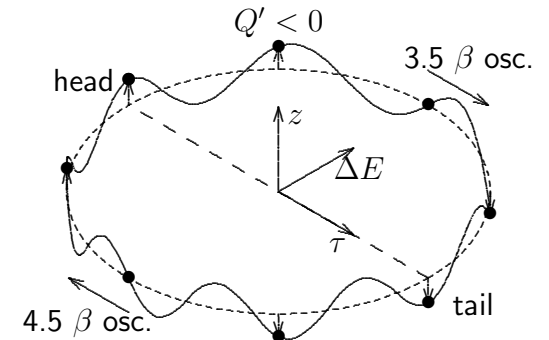
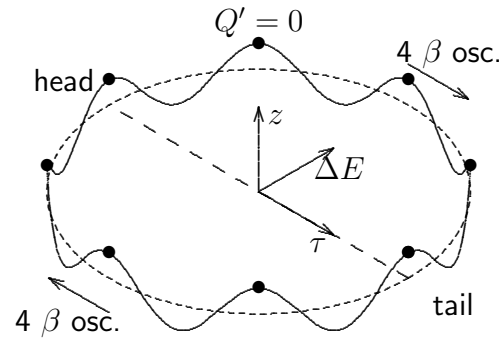
Figure shows betatron motion in steps of its period $T_\beta = T_0/q$.



$$Q' = 0$$

$$Q' > 0$$

CERN booster; Gareyte, Sacherer.



Model of head-tail instability

Above transition energy:

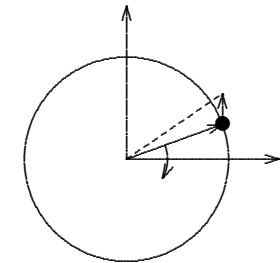
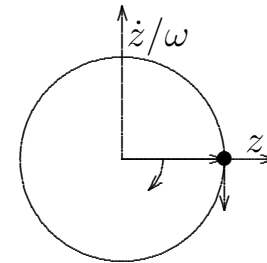
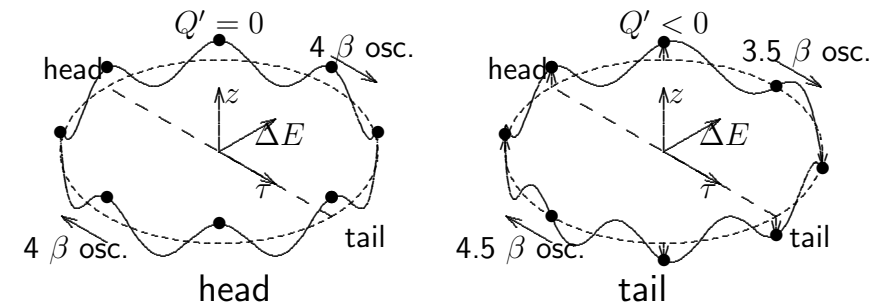
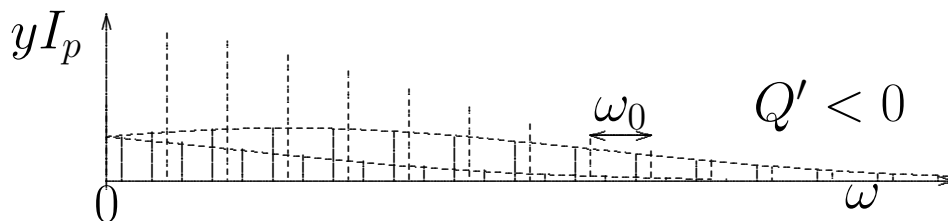
$Q' = 0$: Going from head to tail or from tail to head has same phase change. Phase lag and advance between head and tail interchange, neither damping nor growth.

$Q' < 0$: Going from head to tail there is a loss in phase, going from tail to head a gain (picture), giving a systematic phase advance between head and tail and in average growth.

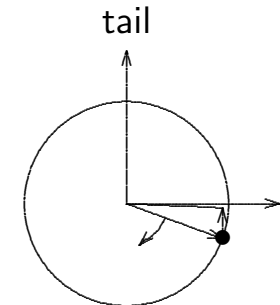
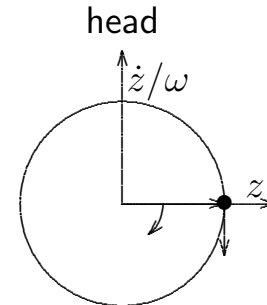
$Q' > 0$: Going from head to tail there is a gain in phase, going from tail to head a loss, giving a systematic phase lag between head and tail and in average damping.

Below transition this situation is reversed.

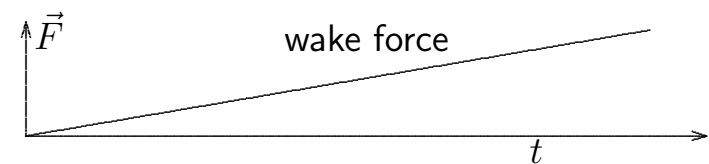
Head tail spectrum:



Tail has phase lag, amplitude is increased



Tail has phase advance, amplitude is decreased

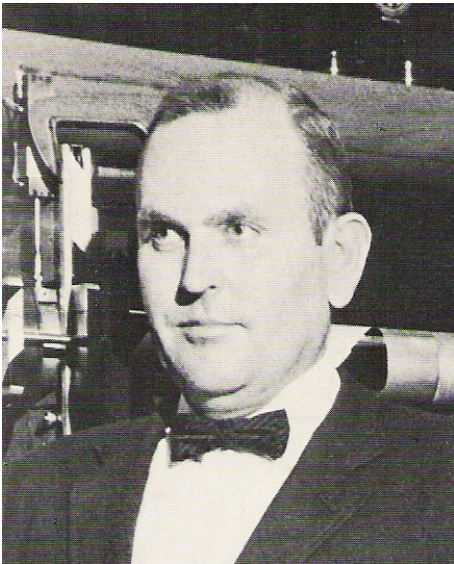


Summary

The instability treatment used here was invented by K. Robinson. This was generalized to nearly all longitudinal and transverse bunched beam instabilities by Frank Sacherer.

This demands for resistive impedance at upper, Z^+ , and lower, Z^- , side-band to fulfill a **stability condition**

	above transition	below transition
longitudinal, stability	$Z_r^+ < Z_r^-$	$Z_r^+ > Z_r^-$
transverse $Q' = 0$, stability	$Z_{Tr}^+ > Z_{Tr}^-$	$Z_{Tr}^+ > Z_{Tr}^-$
transverse head-tail, stability	$Q' > 0$	$Q' < 0$



Ken Robinson



Frank Sacherer